NATURAL CIRCULATION OF WATER AT 1200 PSIA UNDER HEATED, LOCAL BOILING AND BULK BOILING CONDITIONS: TEST DATA AND ANALYSIS

A. S. Rathbun

N. E. Van Huff

A. Weiss

DECEMBER, 1958

ACKNOWLEDGMENT

The authors of this report wish to thank Kurt Katz for his work in the planning and start of this experimental investigation.

SUMMARY

The natural circulation tests performed and analyzed in this report were conducted at 1200 psia on the Bettis Natural Circulation Loop, No. 29. The tests were run with two different single channel test section (0.101 in. x 1 in. x 27 in. long and 0.210 in. x 1 in. x 27 in. long). Heat fluxes ranged from 50,000 Btu/hr-ft^2 to departure from nucleate boiling and inlet subcooling was fixed at 109F$^\circ$.

The results show that there is no difference between natural and forced circulation pressure drop and riser density. (Other tests recently completed but not reported here show similarly that there is no difference between forced circulation and natural circulation DNB providing there are no large deviations of flow due to instabilities.) The tests also show that loop circulating flows in Loop No. 29 can be predicted quite accurately in single phase flow. Circulation rates with two phase flow can be accurately predicted if two phase entrance and exit losses and steam-water slip ratios are known. Further, flow instabilities were noted under certain conditions and occurred before DNB. With the 0.101 in. x 1 in. x 27 in. long test section these instabilities were large enough to cause a DNB. However, at the same conditions no apparent instability was noted with the 0.210 in. x 1 in. x 27 in. long test section.

Some data for slip ratios in two phase flow at inlet velocities less than 1 ft/sec were obtained.

Additional tests with other channel sizes and at other pressures have been completed and data reduction is in progress.

I. INTRODUCTION

In conjunction with the design of the Natural Circulation Reactor plant (NCR) a series of experiments have been planned for the natural circulation loop (Bettis Loop No. 29) of the Bettis Thermal and Hydraulics Laboratory. These experiments are necessary in order to obtain basic information on this mode of circulating coolant. Table I (Ref. 1) outlines the first of these investigations for uniform heat flux in a single channel test section. Heat fluxes range from 50,000 Btu/hr-ft^2 to departure from nucleate boiling (DNB point).

TABLE I

Pressure, psia	Inlet Subcooling		
	109°F	70°F	20°F
800	0.100*	0.100	0.100
	0.200	0.200	0.200
		0.250	0.250
1200	0.100	0.100	0.100
	0.200	0.200	0.200
	0.250	0.250	0.250
1600	0.100		
	0.200	0.200	0.200
2000	0.200	0.200	0.200

*Nominal channel width in inches.

The results reported here are from the first series of these tests covering the following parameters.

Pressure: 1200 psia

Inlet Subcooling: 109°F

Channel Size: 0.100 in. and 0.200 in.

Heat Flux: 50,000 Btu/hr-ft^2 to departure from nucleate boiling.

These experimental data have been analyzed in accordance with the following program objectives:

1. To compare experimental natural and forced circulation pressure drop, DNB, and riser density at the same flow and heat flux.
2. To compare experimental and calculated pressure drops across the test section.
3. To compare experimental natural circulation coolant flow with predicted flow.
4. To examine the effects of varying parameters on natural circulation coolant flow.
5. To examine flow instability and departure from nucleate boiling during natural circulation.

II. DESCRIPTION OF APPARATUS

The tests were conducted in Bettis Loop No. 29, the Natural Circulation Loop, as seen in Fig. 1. The main loop piping is fabricated from schedule 80 type 304 stainless steel, and is in the shape of a vertical rectangle 14.5 ft high and 15 ft long. The test section, as seen in Fig. 1, is mounted at the bottom of one of the vertical legs and discharges into a riser made from 2 in. schedule 80 pipe; the other vertical leg is the downcomer which is 1 1/2 in. schedule 80 pipe. The top horizontal leg consists of a double pipe heat exchanger and by-pass line in parallel; the bottom horizontal leg contains the orifice flowmeter and preheater; both legs are made from 1 1/2 in. schedule 80 pipe. The flanged connections are sealed with Flexitallic gaskets. The auxiliary high pressure systems (manometer connecting lines, degassing lines, ion exchanger lines, etc) are constructed of 1/4 in. and 3/8 in. stainless steel tubing with autoclave fittings and valves. The loop auxiliaries consist of a resin-bed ion exchanger and a pressurizer which are

duplicates of those described in WAPD-188 (Ref. 2). A Westinghouse model 30A, canned-rotor centrifugal pump is connected across a gate valve on the bottom horizontal leg. This pump is used for degassing and de-ionizing the water prior to natural circulation testing and also for forced circulation tests such as isothermal friction factor determination.

Two sizes of rectangular channels were tested. One measured 0.101 in. x 1 in. x 27 in. long and the other 0.210 in. x 1 in. x 27 in. long. The test sections were fabricated of 304 stainless steel and were electrically resistance heated. The channels of both test sections had measured surface finishes of 20 microinches (rms) or less. A detailed explanation of test section fabrication, instrumentation, and its electrical power supply can be found in Chapter II of WAPD-188 (Ref. 2). The pressure tap connections on the test section were spaced 20 and 22 inches apart and are shown in Fig. 1.

III. TEST PROCEDURE

The loop was filled with water, degassed, and de-ionized until the loop water had an O_2 content of less than 0.2 cc/kg and a resistivity not less than one megohm-cm. A series of isothermal pressure drop runs were taken in order to check out the loop and test section instrumentation. The average channel spacing was determined from the isothermal pressure drop data by selecting a channel spacing that would make the measured friction factor coincide with the smooth Moody curve; this is further explained in WAPD-TH-408 (Ref. 3). This spacing was later confirmed by channel probing. The test section and loop instrumentation are similar to that described in Chapter II of WAPD-188 (Ref. 2). In addition to the foregoing instrumentation, differential pressure transducers were placed across the test section and loop flow orifice in order to detect any flow instabilities occurring in the loop.

The natural circulation tests were initiated by setting a specified test section inlet temperature, cold leg temperature, and test section heat flux while the loop was in forced circulation and then stopping and valving off the pump from the loop. Although it was demonstrated that natural circulation start-up was possible, the forced circulation start-up was used to save time in reaching the specified loop temperatures. After the initial start-up the remaining natural circulation tests were run by setting the desired test section heat flux level and then controlling the heat exchanger to give the specified cold leg and inlet temperatures. For each data point obtained the loop was circulated at the specified conditions for a minimum time of one hour. In order to detect loop instabilities the transducers were turned on at the end of each run and allowed to operate until the change of test section heat flux level was completed. The following manometer readings were taken at each heat flux level (see Fig. 1).

TABLE II

Manometer Readings

Test Section Spacing 0.101 in.	Test Section Spacing 0.210 in.	
1-2	1-2	9c-2
10-9a	10-9a	3-1
10-9b	10-9b	10-6
10-9c	10-9c	6-5
4-5	4-5	

IV. EXPERIMENTAL DATA

The data for these tests are tabulated in Appendix B. Tables B-1 and B-3 list the natural circulation data and Tables B-2 and B-4 list the forced circulation data. A routine has been added to the low pressure,

pressure drop code of WAPD-T-663 (Ref. 4) to reduce the data from Loop No. 29. The input to the code is the experimental thermocouple and manometer readings. These readings are reduced to temperature (°F) and pressure drop (PSF). The output of this code directly compares the calculated and experimentally measured test section pressure drops.

All pressure drops shown are negative values, that is, pressure losses. The exit and entrance losses in Tables B-3 and B-4 are the total pressure drop across the exit and entrance flanges, taps 2-9c and 3-1 respectively.

It should be noted that runs 10-1 through 10-6 of Table B-3 were taken at a much later date than the other 0.210 in. data. The increased pressure drop across the entrance is due to a faulty thermocouple which partially blocked off the entrance to the test section in these later runs.

V. ANALYTICAL METHODS

This section contains a discussion of the basic pressure drop equations used in analyzing the experimental data, a discussion of the two-phase G-dependency of the bulk boiling friction factor and the method of predicting natural circulation system flow rate. It should be noted that many of these studies were completed before the issuance of WAPD-TH-410 (Ref. 5).

A. Basic Pressure Drop Equations

The basic pressure drop equations used in this report for the calculations of pressure drop across the test section for single and two-phase flow are presented in WAPD-T-663. In brief, the equations contained in this code are:

1. Heating and Local Boiling Range

$$\Delta P_{fr.H.} = f_{iso} \frac{L}{D_{eq}} \frac{G^2}{2g_c} \frac{1}{\rho_B} \qquad (1)$$

where $f_{iso} = \beta + \frac{\alpha}{N_{Re}^{n}}$

$$\Delta P_{fr.L.} = \frac{G^2}{2g_c D_{eq}} \int_0^L f_{iso} \left(\frac{f}{f_{iso}}\right) \frac{dL}{\rho_B} \qquad (2)$$

where f/f_{iso} plotted versus temperature is defined as a fixed ramp and initiation of local boiling is determined by the Dittus Boelter heat transfer coefficient using a constant of 0.023 and the Jens and Lottes relationship (i.e. $\Delta T_{J\&L} = T_W - T_f$). The acceleration pressure drop for local boiling and heating is given by:

$$\Delta P_{acc.\ H\ and\ L} = \frac{G^2}{g_c} (v_{exit} - v_{in.}) \qquad (3)$$

2. Bulk Boiling Range

$$\Delta P_{fr.B.B} = \frac{G^2 f_{iso \cdot sat}}{2g_c \rho_f D_{eq}} \int_0^L \Phi^2_{Lo_{M\&N}} dL \qquad (4)$$

where $\Phi_{Lo}{}^2{}_{M\&N}$ is the Martinelli and Nelson local two-phase pressure drop ratio. G-dependency of this $\Phi_{Lo}{}^2$ term will be examined in the next section.

Acceleration ΔP is calculated using

$$\Delta P_{acc.B.B} = \frac{G^2}{g_c} v_f \left[\frac{(1-x)^2}{1 - R_g} + \frac{x^2}{R_g} \left(\frac{v_g}{v_f}\right) - 1\right] \qquad (5)$$

where R_g is the void fraction for the modified Martinelli and Nelson separated flow model. Equation (5) is based on a saturated inlet condition and an exit quality x corresponding to a void fraction R_g.

3. Elevation

$$\Delta P_{elev.} = \int_{z=0}^{z=L} \rho \, dz \qquad (6)$$

where $\rho = \rho_f - R_g \rho_{fg}$ in the bulk boiling range, and $\rho = \rho_B$ in the heated and local boiling range.

B. Two-Phase Mass Velocity Dependency

For some time it has been known that there exists a mass velocity dependency on the two-phase friction factor. Ref. 6 described adequately this dependency at 2000 psia. Until recently no similar information has been made available for lower pressures.

Two methods of describing the two-phase friction factor were considered in this study. Initially an interim procedure was used which was found to predict two-phase friction losses 25% too high at the mass velocities of these tests and this error will become larger at lower mass velocities. This dependency was determined arbitrarily from Refs. (6) and (7). The mass velocity dependent Φ_{Lo}^2 was defined as

$$\Phi_{Lo}^2 \underset{\text{for } P_1,\ X_1,\ G_1}{(\text{G-dependent})} = \Phi_{Lo}^2{}_{M \text{ and } N \text{ at } P_1 \text{ and } X_1} \left[\frac{(\Phi_{Lo}^2) \text{ at } G_1}{(\Phi_{Lo}^2)_{G_o}} \right]_{\text{From Ref. (6)}} \quad (7)$$

where $G_o = 1 \times 10^6$ lb/hr ft^2 (Ref. 6). Thus, the mass velocity dependent, Φ_{Lo}^2, at the pressure, flow and quality in question (P_1, x_1, G_1) is found by multiplying the Martinelli and Nelson Φ_{Lo}^2 (at P_1 and x_1) by a ratio of the Φ_{Lo}^2 at the mass velocity in question (G_1) to the Φ_{Lo}^2 at the reference mass velocity. With equation (7) the resultant family of curves at a pressure of 1200 psia could be represented by

$$\Phi_{Lo}^2 \underset{\text{for } P_1}{(\text{G-dependent})} = \frac{Ax}{G^B} + 1 \quad (8)$$

with A and B as arbitrary constants.

An experimentally verified relation for this mass dependency has been recently described in Ref. (5). This relation was determined from overall pressure drop data taken at pressures from 400 to 1600 psia on a 22 in.

length of a 0.097 in. x 1 in. x 27 in. long rectangular channel test section and across a 60 in. length of a 0.070 in. x 2.25 in. x 72 in. long test specimen at a wide range of heat fluxes, mass velocities, and inlet temperatures. The friction pressure drop was determined by subtracting from the total pressure drop the acceleration and elevation pressure drop which were determined from the modified Martinelli and Nelson void fractions (Ref. 8). The actual two-phase friction factor ratio Φ_{Lo}^2 was found and the best estimate of these data is given in the form of a multiplier for the normal Martinelli and Nelson local two-phase friction factor (Ref. 7).

For mass velocities $\leq 0.7 \times 10^6$ lb/hr-ft^2, use

$$\frac{\Phi_{Lo}^2}{\Phi_{Lo}^2}_{M \text{ and } N} = 1.36 + 0.0005\,P + 0.1\,\frac{G}{10^6} - 0.000714\,P\,\frac{G}{10^6} \qquad (9)$$

and for mass velocities $\geq 0.7 \times 10^6$ lb/hr-ft^2, use

$$\frac{\Phi_{Lo}^2}{\Phi_{Lo}^2}_{M \text{ and } N} = 1.26 - 0.0004\,P + 0.119\,\left(\frac{10^6}{G}\right) + 0.00028\,P\,\left(\frac{10^6}{G}\right) \qquad (10)$$

The detailed analysis in this report uses equations (9) and (10) which have been introduced into the low pressure, pressure drop code previously mentioned.

C. System Performance

In order to predict the coolant flow rate for a natural circulation system, a knowledge of the pressure drop around the entire loop is necessary. For a given heat input and heat extraction, the flow in the loop will be that value where the frictional and acceleration losses around the loop are equal to the difference in elevation head between the hot and cold portion of the loop.

$$\Delta P_{elev_{loop}} + \Delta P_{acc_{loop}} + \Delta P_{fr_{loop}} = 0 \qquad (11)$$

The following section discusses these pressure drops with respect to Loop No. 29.

1. Elevation Pressure Drop

The elevation term, or thermal driving head, of equation (11) is given by

$$\Delta P_{elev_{loop}} = \sum_{i=1}^{n}{}_{cl} \rho_i \Delta z_i - \sum_{i=1}^{n}{}_{hl} \rho_i \Delta z_i \qquad (12)$$

The single-phase densities for equation (12) are easily determined from knowledge of the system pressure and fluid temperature. The densities in the two-phase regions are more difficult to evaluate because of the varying slip ratios (vapor velocity to fluid velocity) in these regions.

In the test section and the exit flange, two-phase densities are calculated using

$$\rho = \rho_f - R_g \rho_{fg} \qquad (13)$$

where R_g, the void fraction, is obtained from the modified Martinelli and Nelson curves (Ref. 8). This assumption is based on the limited information available for slip ratios at the inlet fluid velocities encountered in the test section (1.5 ft/sec to 3 ft/sec). These can be justified using the experimental curves of slip ratio vs pressure for various inlet velocities found on pg 30 of Ref. (9) and comparing it with the calculated modified Martinelli and Nelson slip ratio shown on pg 10 of Ref. (4).

Most of the elevation head difference in the loop is due to the 2 in. riser above the test section, and at present few data are available on the values of slip ratios for the relatively low fluid velocities in the riser, 0.1 to 0.5 ft/sec. Evaluation of slip ratio vs fluid velocity

and quality was a necessary step in examining system performance. This information could be obtained from pressure drop measurements across the riser for each run. Equating the pressure drops across the riser and solving for ρ results in

$$\rho = \frac{\Delta P_{measured} - \Delta P_{fr}}{L} \tag{14}$$

if the heat losses in the riser are negligible. Calculation of the heat losses amount to a maximum change in the slip ratio of 1.5% at 15% quality which is considered negligible to the overall system performance.

Equation (15) is the definition of void fraction,

$$\rho = \rho_f - R_g \rho_{fg} \tag{15}$$

and equation (16) shows the void fraction as a function of slip ratio.

$$R_g = \frac{1}{\frac{V_g/V_f}{v_g/v_f}\left(\frac{1-x}{x}\right) + 1} \tag{16}$$

Equations (14), (15), and (16) can be rearranged and solved for slip ratio, resulting in equation (17).

$$V_g/V_f = \frac{v_g}{v_f}\left(\frac{x}{1-x}\right)\left[\frac{\rho_{fg}}{\rho_f - \frac{\Delta P_{meas} - \Delta P_{fr}}{L}} - 1\right] \tag{17}$$

The magnitude of the frictional pressure drop in the riser was found to be negligible compared to the elevation pressure drop.

Experimental slip ratios calculated from equation (17) are plotted on Fig. 2 for the natural circulation and forced circulation runs reported in Appendix B. As the velocities in the riser become smaller, the effect of quality on the slip ratio in the range tested is apparently small.

2. Acceleration Pressure Drop

The acceleration pressure drop due to area and density changes was summed up around the loop and the resulting acceleration loss is

$$\Delta P_{\substack{acc \\ loop}} = \frac{W^2}{2gA_{ts}^2}\left[\frac{1}{\rho_a} - \frac{1}{\rho_{cl}}\right] + \frac{W^2}{2gA_{he}^2}\left[\frac{1}{\rho_{cl}} - \frac{1}{\rho_{sr}}\right]$$

$$+ \frac{W^2}{2gA_rA_a}\left[\frac{1}{\rho_r} - \frac{1}{\rho_a}\right] + \frac{W^2}{2gA_rA_{he}}\left[\frac{1}{\rho_{sr}} - \frac{1}{\rho_r}\right] \qquad (18)$$

This equation is derived in Appendix A.

3. Friction Pressure Drops

The four major friction pressure drops, accounting for 99% of the total friction loss, occur across the orifice, the test section itself and the entrance and the exit flanges of the test section. These pressure drops for the 0.101 in. and the 0.210 in. channel are tabulated in Table III for two runs of approximately the same exit quality.

a. Orifice

The pressure drop for the orifice in the loop is given by

$$\Delta P = \frac{K}{2g A_p^2}\frac{W^2}{\rho_{cl}} = 0.008\frac{W^2}{\rho_{cl}} \qquad (19)$$

The experimental results indicate that none of the pressure drop across the orifice is recovered downstream from the orifice.

TABLE III

0.101 in. x 1.0 in. x 27 in. Channel

W = 349 lb/hr (G = 0.5 x 10^6 lb/hr-ft^2)

ϕ = 305,000 Btu/hr-ft^2

X_{exit} = 0.275

Loop Losses	psf
Orifice	19.0
Entrance	7.4
Test Section	110.4
Exit	122.8
Loop Friction (Other)	1.0-
Acceleration Loss	21.0
Total	281.6

0.210 x 1.0 in. x 27 in. Channel

W = 697 lb/hr ($G = 0.5 \times 10^6$ lb/hr-ft^2)

$\dot{Q}$ = 562,000 Btu/hr-ft^2

X_{exit} = 0.253

Loop Losses	psf
Orifice	75.9
Entrance	25.6
Test Section	43.7
Exit	90.6
Loop Friction (Other)	1.0-
Acceleration Loss	15.0
Total	251.8

b. Test Section

The friction loss across the test section is calculated from the low pressure, pressure drop code of WAPD-T-663 combined with the recent two-phase G-dependency of Ref. (5).

c. Entrance Flange

The configuration of the entrance flange is shown in Fig. 1. The loss from taps 1-3 (Fig. 1) is given by

$$\Delta P_{ent} = \frac{K_{ent} W^2}{2g_c \rho_{cl} A^2_{ts}} \tag{20}$$

where $K_{\substack{ent \\ exit}}$ is defined as

$$K_{\substack{ent \\ exit}} = A^2_{ts} \sum_i^n \frac{K_i}{A_i^2} + A^2_{ts} \sum_i^n \frac{f L_i}{D_{e_i} A_i^2} \tag{21}$$

The K_i values of (21) are the single-phase expansion and contraction losses taken from Ref. (10).

Table IV lists the calculated and measured values of the entrance K-factor. The 0.210 in. test section measured value was determined from the isothermal runs. No measured value was available for the smaller channel. The large discrepancy between the calculated and measured value for the large channel is believed due to the faulty thermocouple. The measured values were used in all the calculations for this report.

TABLE IV

$K_{entrance}$

Test Section	Calculated	Measured
0.101 in.	0.8	---
0.210 in.	2.1	3.8

d. Exit Flange

Lack of an experimentally verified relation to calculate two-phase contraction and expansion losses makes the calculation across the exit flange (taps 2 to 9c) more difficult. Since at 1200 psia fog flow has been determined to be inaccurate, this method of calculating the two-phase exit losses is not considered. The friction pressure drop is determined by subtracting the acceleration and elevation pressure drops, calculated

using the modified Martinelli and Nelson void fractions, from the total pressure drop across the exit. The resulting experimental friction pressure drop is examined by three methods of calculation.

Method 1 is based on the two-phase fluid density,

$$\Delta P = \frac{K_{exit} W^2}{2 g_c A_{ts}^2 \rho_{M\&N}} = \left(\frac{\rho_f}{\rho_{M\&N}}\right) \frac{K_{exit} W^2}{2 g_c A_{ts}^2 \rho_f} \qquad (22)$$

where the two-phase fluid density is that calculated from the modified Martinelli-Nelson void fraction curves and K_{exit} is the same as that used for single-phase flow.

Method 2 is based on the Martinelli-Nelson two-phase multiplier. Since two-phase friction losses are adequately described by a multiplier, it seems logical that two-phase exit losses might also be described using a multiplier as shown in (23).

$$\Delta P = \Phi_{Lo}^2 \frac{K_{exit} W^2}{2 g_c A_{ts}^2 \rho_f} \qquad (23)$$

Method 3 is derived from the experimental measurements across the exit flange, taps 2-9c, Fig. 1.

$$\Delta P = \left[\frac{K_{tpf}}{K_{exit}}\right] \frac{K_{exit} W^2}{2 g_c A_{ts}^2 \rho_f} \qquad (24)$$

The calculated single-phase exit K-factor (found from equation 21) and measured values (from isothermal runs) are shown in Table V for the two channel sizes.

TABLE V

	K_{exit}	
Test Section	Calculated	Measured
0.101 in.	1.2	---
0.210 in.	2.9	3.2

The calculated values of $\frac{\rho_f}{\rho_{M\&N}}$, Φ_{Lo}^2, and $\frac{K_{tpf}}{K_{exit}}$ as a function of quality at 1200 psia are shown on Fig. 3. The experimental factor is determined from

$$\frac{K_{tpf}}{K_{exit}} = \frac{\Delta P_{fr\ exit}}{\left[\frac{K_{exit}\ W^2}{2g_c\ \rho_{sat}}\right]} \tag{25}$$

where

$$\Delta P_{fr_{exit}} = \Delta P_{\substack{meas \\ 9c-2}} - \Delta P_{elev} - \Delta P_{acc.} \tag{26}$$

The elevation loss term in equation (26) is given by

$$\Delta P_{ele} = \rho_{M\&N} Z_{\substack{TAP\ 2 \\ to\ beginning \\ of\ riser}} + \rho_r Z_{\substack{beginning \\ of\ riser \\ to\ tap\ 9c}} \tag{27}$$

and the acceleration loss is given by the relationship derived in Appendix A, i.e.:

$$\Delta P_{\substack{ACC \\ 2-9c}} = \frac{W^2}{2g_c}\left[\frac{1}{A_r} + \frac{1}{A_{ts}}\right]\left[\frac{1}{\rho_r A_r} - \frac{1}{\rho_{M\&N} A_{ts}}\right] \tag{28}$$

Note that the acceleration pressure drop from equation (28) gives a pressure rise for the exit configuration.

Fig. 4 also compares the relative magnitudes of these three methods for various qualities. The experimental method is intermediate to the other two. Fig. 4 compares the measured total pressure drop across the exit with the calculated values. It can be seen that at the higher qualities the density method calculated total loss up to 40% too low, while the multiplier method calculates losses up to 30% too high. The

experimental method as expected predicts the value almost exactly. It will be shown later that the method chosen to calculate the exit loss has a large effect on the accuracy of the flow prediction of this loop.

VI. DATA ANALYSIS

A. Test Section Pressure Drop

1. Comparison of Forced and Natural Circulation

Initially, because of the difference of the driving force in natural and forced circulation it was necessary to determine if there was any difference in the pressure drops for these two modes of operation for a given heat flux and system flow. The oscillatory behavior of the loop with the 0.101 in. test section during natural circulation operation limits comparison of data for this test section to heat fluxes less than 320,000 Btu/hr-ft^2. For the 0.210 in. test section comparisons are made up to the DNB heat flux of 890,000 Btu/hr-ft^2.

Fig. 5 is a plot of total measured pressure drop across the test section versus heat flux. For the 0.101 in. channel, a few of the natural circulation points were duplicated with forced circulation, while every 0.210 in. natural circulation run was duplicated. The plot of these points indicates that no significant difference in test section pressure drop is evident between the two modes of operation up to a point of instability and/or departure from nucleate boiling. This agreement holds over wide ranges of exit quality, from 0 to 30% in the 0.100 in. channel and from 0 to 55% in the 0.210 in. channel.

A further comparison to substantiate this conclusion can be made for the riser density. Fig. 6 is a plot of riser density versus heat flux for the 0.210 in. for the two modes of operation. It is clearly shown again that no significant difference can be noted between natural and forced circulation.

2. Experimental vs Calculated Pressure Drop

Fig. 7 shows a comparison between the experimental and calculated values of total pressure drop across the two test sections. The two-phase friction loss was calculated using the latest relationship as described by equations (9) and (10). The calculated value is within 10% of the measured value for all exit qualities.

Figs. 8, 9, 10, and 11 display the comparison between the calculated and measured friction pressure drops with and without the use of a mass velocity dependent friction factor. Both the calculated and measured values were determined by subtracting from the total pressure drop the calculated acceleration and elevation pressure drops using the modified Martinelli-Nelson void fractions. Figs. 8 and 9 are a comparison without a mass velocity dependent two-phase friction factor while Figs. 10 and 11 are the same plots using the mass velocity dependency of equations (9) and (10). The purpose for showing Figs. 8 and 9 is to emphasize the discrepancy which can occur if the mass velocity effect is not considered. The experimental points include no boiling, local boiling, and bulk boiling regions with exit qualities up to 50%.

The measured values of ΔP_{fr} for the 0.101 in. test section (Fig. 11), using the mass velocity dependency of equations (9) and (10), are within 10% of the predicted values in the bulk boiling region. The calculated losses are slightly higher than the experimental losses. Without the G-dependency, calculated friction values are predicted as much as 35% too low. In the local boiling regions, the calculated pressure drops are higher than measured as would be expected from the local boiling fixed ramp relation used to calculate this pressure drop. In the heated range, the friction pressure

drop is predicted to within 10%. Equation (8) (the interim G-dependency correlation) predicts a 25% greater pressure drop than was measured for the higher qualities and at the mass velocities of these tests. This difference becomes much greater at lower mass velocities.

The 0.210 in. channel results show more scatter and somewhat larger errors than the 0.101 in. channel results. The calculated losses are consistently lower than the experimental results with errors generally less than 20% for all qualities using the G-dependency relationships. Without this dependency, the calculated friction loss is as much as 50% less than the experimental value (see Fig. 9).

The agreement between the experimental and calculated values using the G-dependency correlation defined in (9) and (10) is very good and within the quoted accuracy of the empirical equations. An interesting point though is that the 0.101 in. pressure drop predictions are consistently conservative while the 0.210 in. are consistently not conservative. The reason for this is not readily apparent and more data are desirable to confirm any definite trend.

3. System Flow

Fig. 12 shows the measured flow rate versus heat flux for both test sections. The flow-flux curve for each test section follows a similar pattern, first increasing in flow up to exit qualities of about 20% and then decreasing to a point of instability and/or a departure from nucleate boiling. The flow decrease is a result of the large frictional and acceleration losses at high qualities exceeding the increased driving head at this quality.

The comparison of the predicted and calculated flow-flux curves (using the three methods for calculating exit losses) is shown in Fig. 13. These prediction curves were obtained by plotting the thermal head curve

vs flow rate and the loop loss curve vs flow rate for various heat fluxes. The intersections of these curves indicate the predicted flow-flux curve. An example is shown in Fig. 14 for the 0.210 in. channel using G-dependency and Method 3 (the experimental multiplier) for calculating the exit flange losses. The results of this comparison are consistent with the discussion on the three methods for predicting exit losses. With single-phase conditions, the predicted flow is within 5% of the experimental flow and each calculated curve is identical up to 0% quality and diverge with increasing quality. All three methods predict the trend of the flux-flow curve but vary markedly in accuracy of prediction. Method 1 predicts flows up to 20% too high and Method 2 predicts flows up to 15% too low. Method 3 gives excellent agreement for both channel sizes with errors less than 5% for all qualities.

Only the flow prediction using the experimentally determined exit loss can be considered good. These results indicate that neither Method 1 nor Method 2 is adequate for use in predicting system flow for qualities greater than 15%. Also, it can be pointed out that the accuracy in calculating the system flow is not necessarily an indication that the correlations employed are accurate. The chance for cancellation of errors is great since so many components are involved. It is, therefore, the prediction of the pressure drop across these individual components that is the true measure of accurate prediction. For this reason development of adequate theory and more experimental verification for predicting two-phase densities and two-phase exit and entrance losses are needed for accurate predictions of flow in a natural circulation system with two-phase losses.

4. Natural Circulation Loop Behavior for 0.101 in. and 0.210 in. Test Sections

A remarkable difference in the loop behavior between the two channel sizes is apparent. The most obvious differences resulting from replacing the 0.101 in. channel with the 0.210 in. while keeping all other parameters constant are:

(1) The maximum flow is increased from 400 to 700 lbs/hr.

(2) The heat flux before reaching departure from nucleate boiling is increased from 300,000 to 900,000 Btu/hr-ft^2.

(3) The 0.101 in. channel flow oscillated at high qualities while the 0.210 in. channel flow did not.

The increase in flow is a direct result of the decreased friction loss in the wider channel. Table III is a comparison of the four major losses for the two channel sizes at 25% exit quality. Whereas, the test section loss is 40% of the total friction and acceleration loss in the small channel, this loss is only 18% in the large channel. It should be noted, however, that in this loop an increase in channel size, to say 0.400 in., will not result in a similar percentage increase in flow because the orifice becomes the flow-limiting loop pressure loss.

The low terminating flux in the 0.101 in. channel is a direct result of the flow oscillations which occurred. These oscillations were not apparent during the forced circulation runs or during tests with the large channel. This large amplitude oscillation of the flow occurred at a heat flux level of 320,000 Btu/hr-ft^2 and a flow of 330 lb/hr at 1200 psia and 109°F subcooled. The exit quality at these conditions was 32%. The type of oscillations are shown in Fig. 15. No oscillations were noted at heat fluxes lower than this. Because of the low value of flow over a portion

of the cycle, departure from nucleate boiling occurred as soon as oscillation began. However, the temperature of the surface did not rapidly increase but only gradually increased. The increase of flow over part of the cycle is enough to carry away some of the heat and modify the resulting temperature rise at the surface.

VII. CONCLUSIONS

The following conclusions can be drawn from this experimental investigation of fluid flow in a single channel test section with uniform heat flux.

A. Natural versus Forced Circulation Performance

1. If no flow instabilities occur, there is no apparent difference between forced or natural circulation pressure drops for identical thermal fluid conditions.

2. Flow instabilities can occur in two-phase natural circulation flow which are not apparent during forced circulation flow at the same conditions.

B. Experimental versus Calculated Pressure Drops

1. The total pressure drop across the 0.101 in. x 1 in. x 27 in. and the 0.210 in. x 1 in. x 27 in. long test sections, using the pressure drop equations in WAPD-T-663, modified by the recommendation of WAPD-TH-410, is predicted to be within $\pm$10% for the bulk boiling region up to qualities of 50%. In the local boiling region the calculated total pressure was 20% higher than the measured values. The heated region calculated total pressure drop was within $\pm$10% of that measured.

2. The use of the mass velocity dependency correction on the two-phase friction factor is required to predict adequately two-phase pressure drops. The G-dependency correlations of WAPD-TH-410 predict the test section friction losses within $\pm$20% for the conditions studied.

3. The use of the Martinelli-Nelson two-phase multiplier to calculate two-phase contraction and expansion friction losses predicts pressure drops up to 30% too high at 55% quality.

The same losses predicted by using the Martinelli-Nelson two-phase densities are 30% too low at 55% quality. For qualities less than 10% this relation is adequate for these calculations.

A two-phase multiplier $(\frac{K_{tpf}}{K_{ex}})$ has been calculated from the experimental data which accurately predicts the exit contraction and expansion losses for Loop No. 29. This multiplier gives friction losses intermediate to the two methods above as shown in Fig. 4.

4. The existence of extremely high slip ratios (up to 16) were observed with two-phase flow at the very low flow rates occurring in the riser. Knowledge of slip ratio is essential to the calculation of the elevation pressure drop and therefore to the prediction of natural circulation performance. Slip ratio vs saturated inlet velocity for the tests of this report are shown in Fig. 3.

C. System Flow

1. Single-phase natural circulation flow can be predicted within 5% using the methods presented in this report.

2. Increasing the channel spacing from 0.101 in. to 0.210 in. without changing the external loop resulted in an increase of flow from 400 lb/hr to 700 lb/hr. This increase, however, is not proportional to the change in channel size.

3. Two-phase natural circulation flow can be predicted to within ±5% if two-phase contraction and expansion losses can be adequately described and if the density in the hot leg of the loop can be determined.

4. Accurate prediction of individual component pressure drops is required in order to assure valid prediction of natural circulation system flow.

D. Flow Instability and Departure from Nucleate Boiling

1. With the 0.101 in. x 1 in. x 27 in. test section the maximum heat flux obtained before an instability occurred, which in turn caused a departure from nucleate boiling, was 320,000 Btu/hr-ft^2.

2. With the 0.210 in. x 1 in. x 27 in. test section no sign of an instability was noted up to a heat flux of 900,000 Btu/hr-ft^2 where departure from nucleate boiling was observed.

NOMENCLATURE

A	-	area (ft^2)
D_{eq}	-	equivalent diameter (ft)
f_{iso}	-	isothermal friction factor
G	-	mass velocity ($lb/hr\text{-}ft^2$)
g_c	-	acceleration due to gravity (ft/hr^2)
L	-	length (ft)
ΔP	-	pressure drop (lb/ft^2)
P	-	system pressure (psi)
R_g	-	void fraction ($\frac{ft^3 \text{ steam}}{ft^3 \text{ mixture}}$)
V	-	velocity (ft/hr)
v	-	specific volume (ft^3/lb)
W	-	weight flow (lb/hr)
x	-	quality ($\frac{lb \text{ steam}}{lb \text{ mixture}}$)
ρ	-	density (lb/ft^3)
Φ_{Lo}^2	-	two-phase friction multiplier
β, α, n	-	constants in f_{iso} equation

Subscripts

acc	-	acceleration
a	-	exit and entrance flange
B	-	bulk
BB	-	bulk boiling
cl	-	cold leg
elev	-	elevation
ent	-	entrance

NOMENCLATURE

(Continued)

fr	-	friction
f	-	saturated liquid
fg	-	saturated liquid-saturated gas transition
g	-	saturated gas
he	-	heat exchanger
H	-	heated region
in	-	in
L	-	local boiling
M&N	-	Martinelli and Nelson
P	-	1 1/2" pipe (hot leg)
r	-	riser
tpf	-	two-phase flow
ts	-	test section
w	-	wall
sr	-	small riser

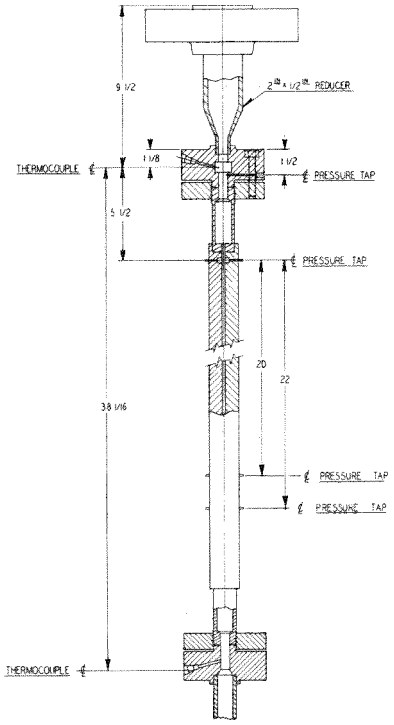

ENLARGED PORTION OF TEST SECTION LEG
VIEW A-A
SCALE 1/2" = 1"

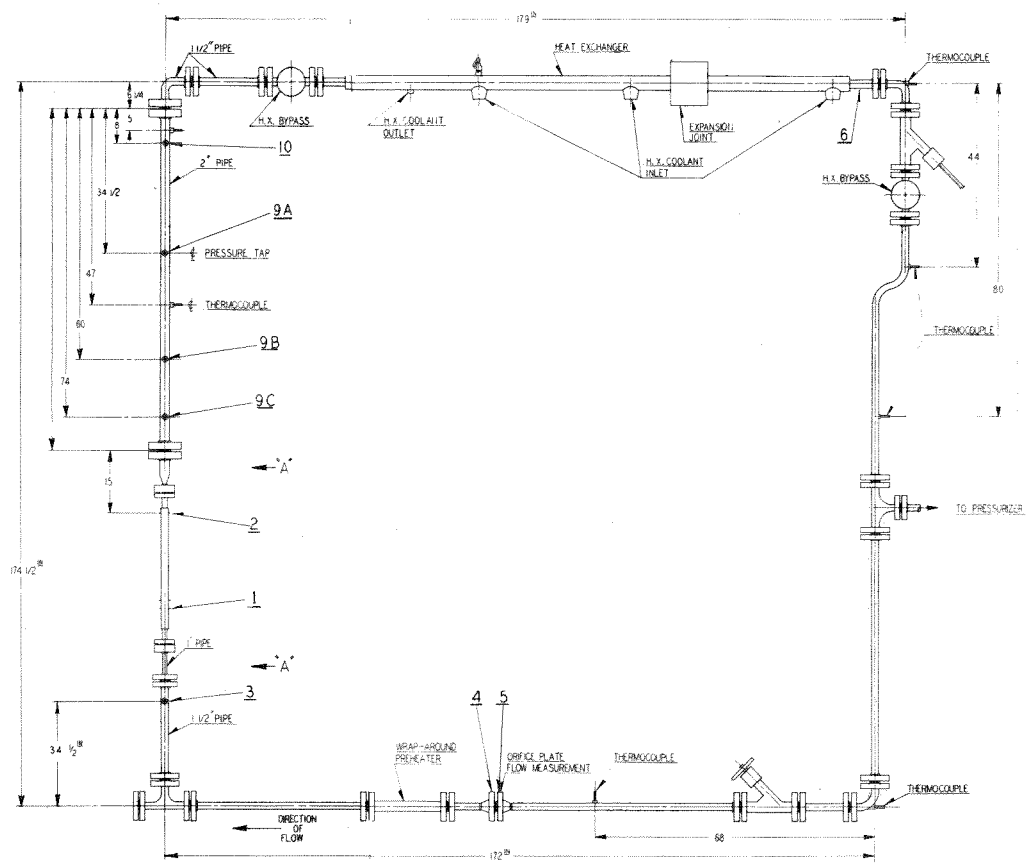

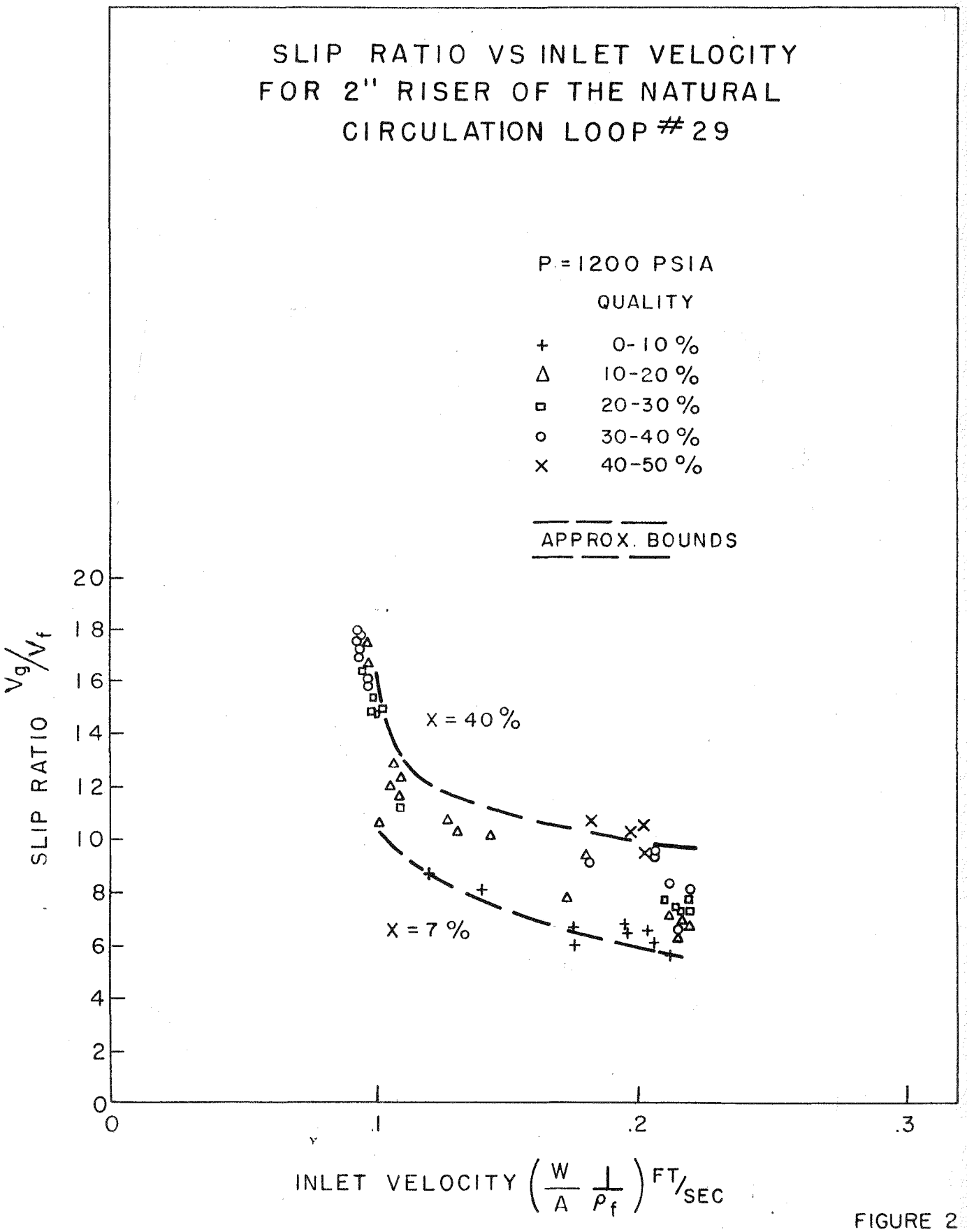

FIGURE 2

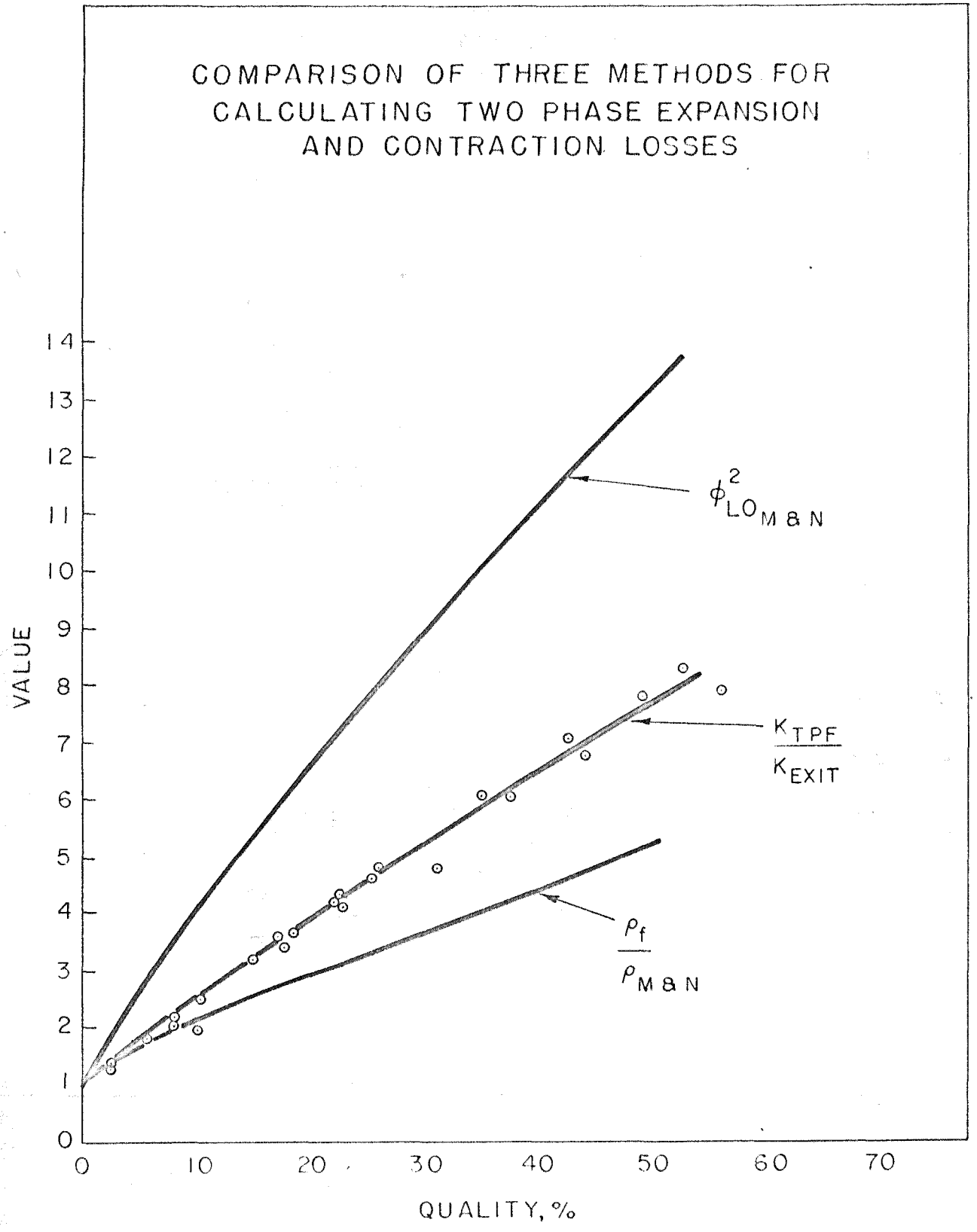

FIGURE 3

EXPERIMENTAL VS CALCULATED TOTAL PRESSURE DROP FROM TAPS 2-9c(EXIT) FOR THREE METHODS OF PREDICTING EXIT LOSSES

▲ METHOD 1 $\Delta P_{FR} = \left(\frac{\rho_f}{\rho_{M\&N}}\right) \frac{K_{EXIT} W^2}{2 g_c A_{TS}^2 \rho_f}$

× METHOD 2 $\Delta P_{FR} = \phi_{LO}^2 \frac{K_{EXIT} W^2}{2 g_c A_{TS}^2 \rho_f}$.

o METHOD 3 $\Delta P_{FR} = \left(\frac{K}{K_{EXIT}}\right) \frac{K_{EXIT} W^2}{2 g_c A_{TS}^2 \rho_f}$

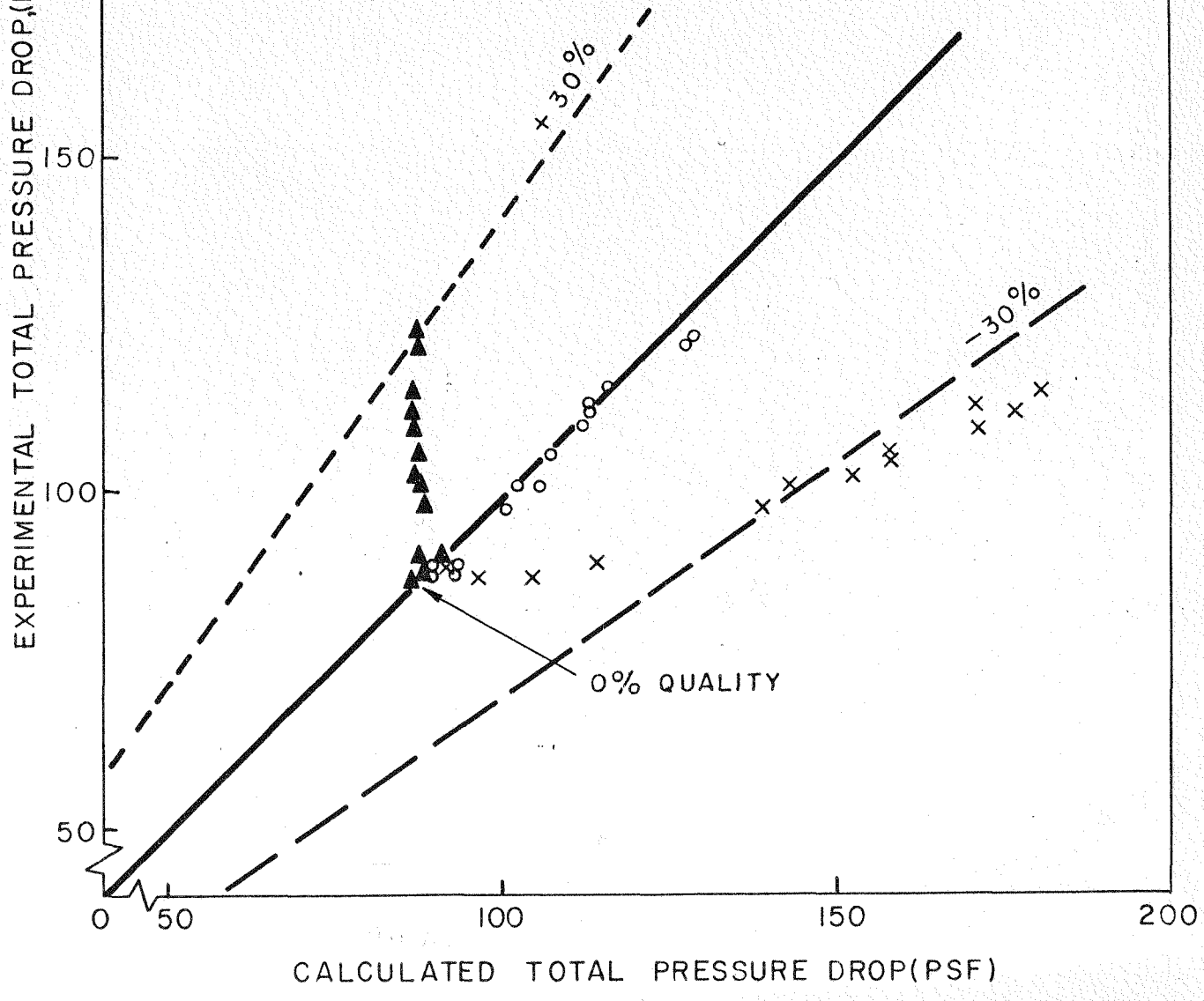

FIGURE 4

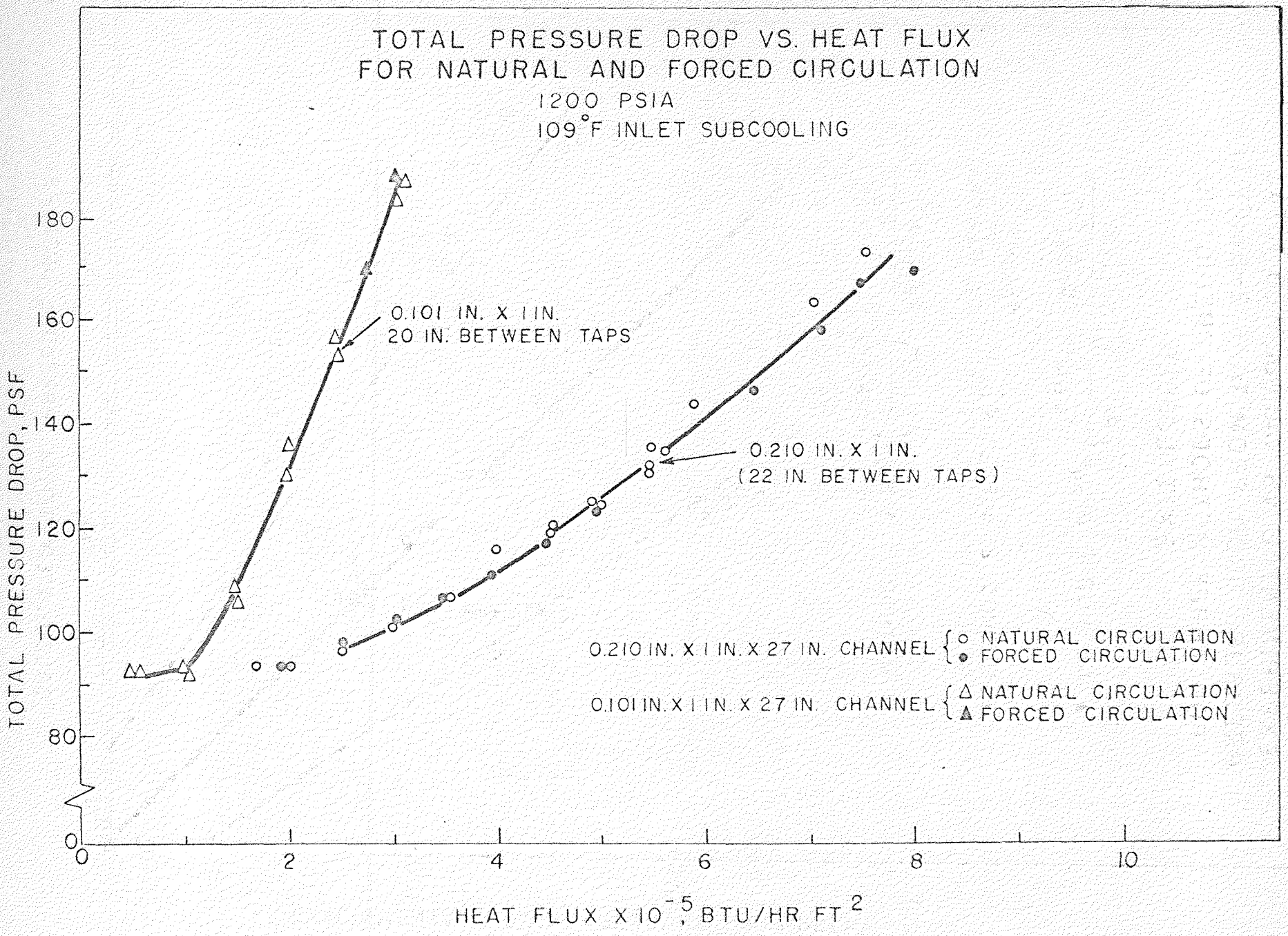
TOTAL PRESSURE DROP VS. HEAT FLUX
FOR NATURAL AND FORCED CIRCULATION
1200 PSIA
109°F INLET SUBCOOLING
TOTAL PRESSURE DROP, PSF
180
160
140
120
100
80
0
0.101 IN. X 1 IN.
20 IN. BETWEEN TAPS
0.210 IN. X 1 IN.
(22 IN. BETWEEN TAPS)
0.210 IN. X 1 IN. X 27 IN. CHANNEL
NATURAL CIRCULATION
FORCED CIRCULATION
0.101 IN. X 1 IN. X 27 IN. CHANNEL
NATURAL CIRCULATION
FORCED CIRCULATION
0
2
4
6
8
10
HEAT FLUX X 10⁻⁵, BTU/HR FT²

FIGURE 5

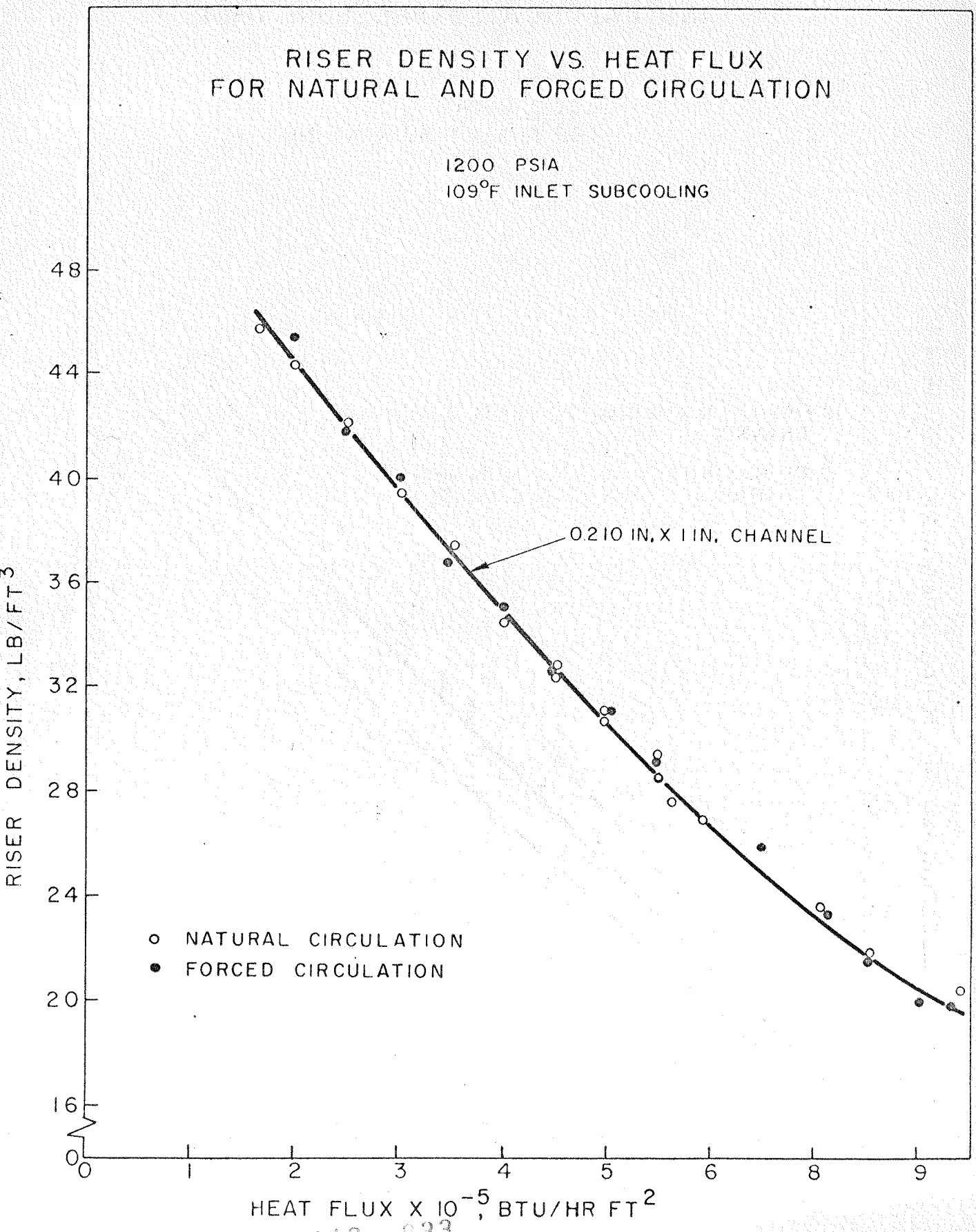

FIGURE 6

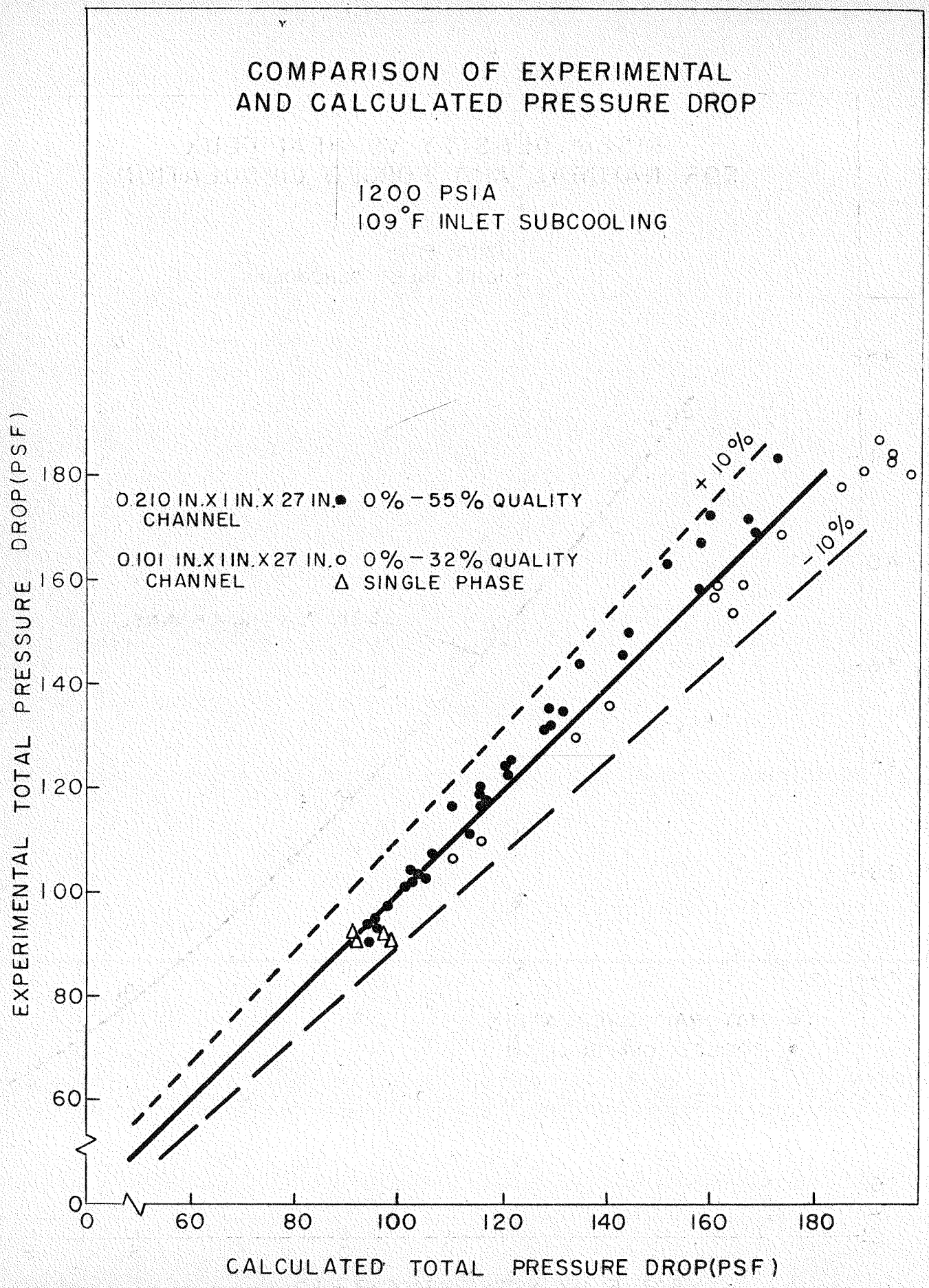
COMPARISON OF EXPERIMENTAL
AND CALCULATED PRESSURE DROP
1200 PSIA
109°F INLET SUBCOOLING
0.210 IN.X1 IN.X 27 IN. CHANNEL
0% – 55% QUALITY
0.101 IN.X1IN.X27 IN. CHANNEL
0% – 32% QUALITY
Δ SINGLE PHASE
+10%
-10%
EXPERIMENTAL TOTAL PRESSURE DROP(PSF)
CALCULATED TOTAL PRESSURE DROP(PSF)
0
60
80
100
120
140
160
180

FIGURE 7

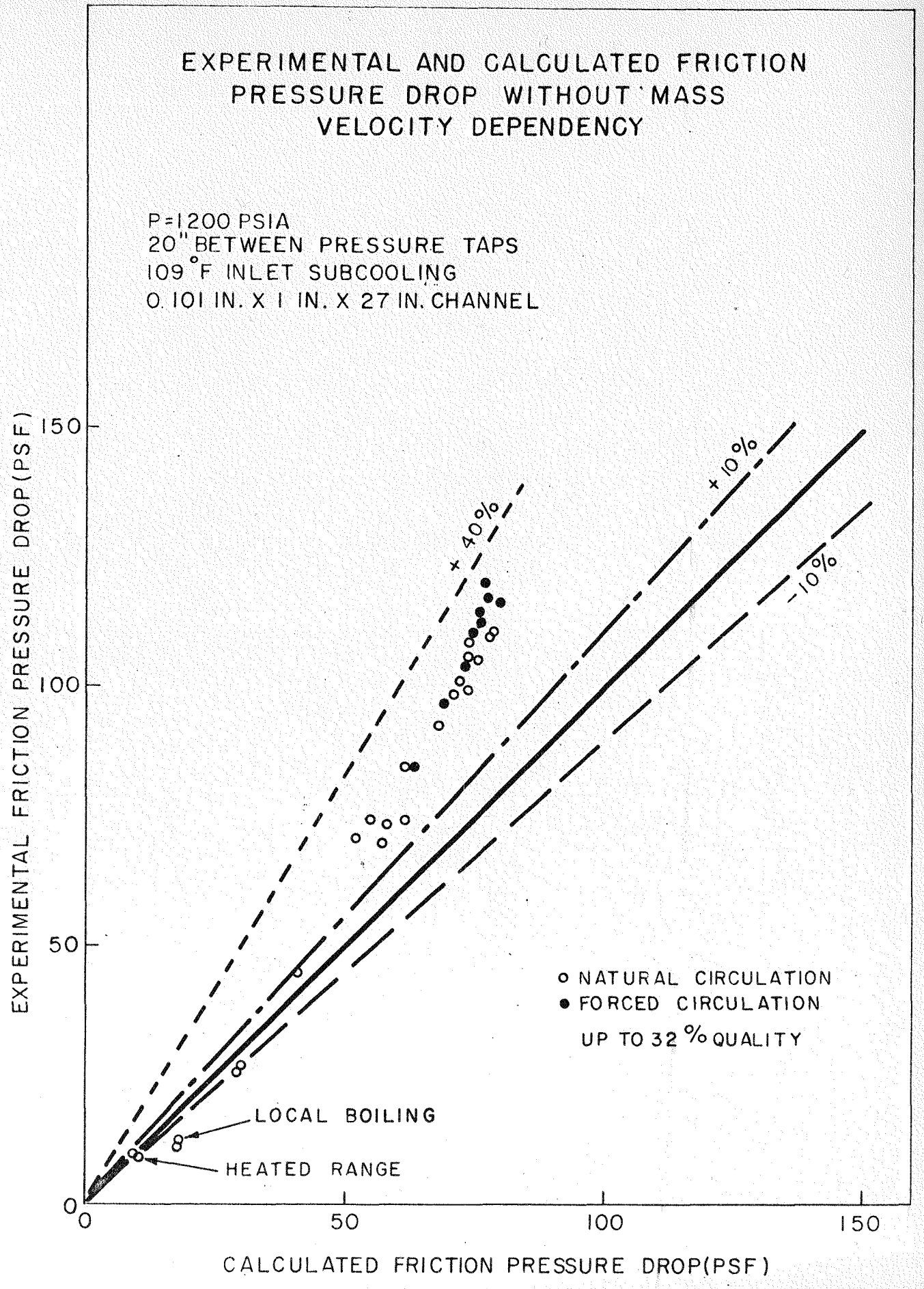
EXPERIMENTAL AND CALCULATED FRICTION PRESSURE DROP WITHOUT MASS VELOCITY DEPENDENCY
P=1200 PSIA
20" BETWEEN PRESSURE TAPS
109 °F INLET SUBCOOLING
0.101 IN. X 1 IN. X 27 IN. CHANNEL
EXPERIMENTAL FRICTION PRESSURE DROP (PSF)
CALCULATED FRICTION PRESSURE DROP (PSF)
0
50
100
150
+40%
+10%
-10%
o NATURAL CIRCULATION
• FORCED CIRCULATION
UP TO 32 % QUALITY
LOCAL BOILING
HEATED RANGE

FIGURE 8

EXPERIMENTAL VS. CALCULATED FRICTION PRESSURE DROP WITHOUT MASS VELOCITY DEPENDENCY

P=1200 PSIA
22" BETWEEN PRESSURE TAPS
109 °F INLET SUBCOOLING
0.210 IN. X 1.0 IN. X 27 IN. CHANNEL

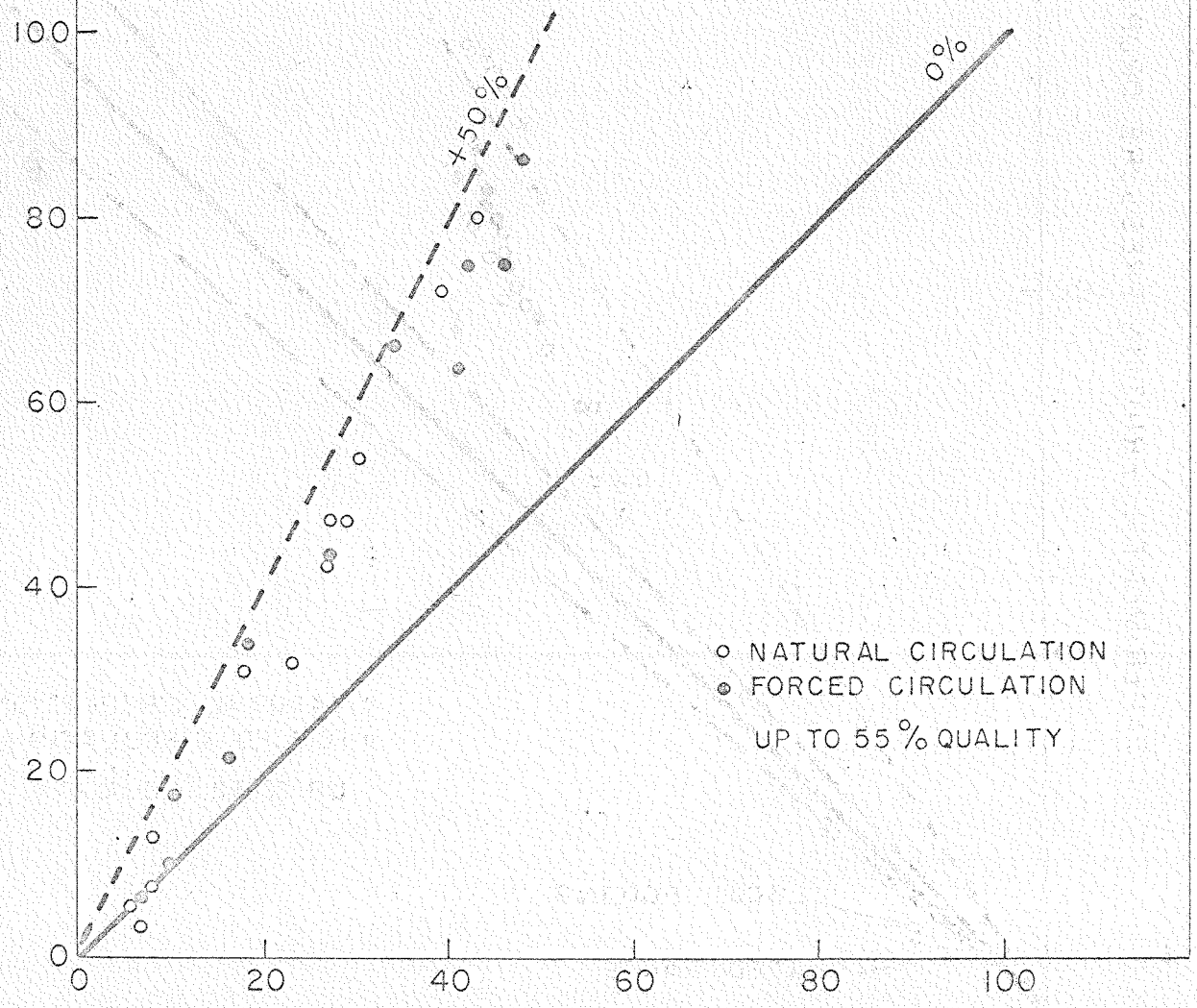

FIGURE 9

EXPERIMENTAL AND CALCULATED FRICTION PRESSURE DROP WITH A MASS VELOCITY DEPENDENCY

P=1200 PSIA
20" BETWEEN PRESSURE TAPS
109°F INLET SUBCOOLING
.101"X1"X27" CHANNEL

$$\frac{\phi_{LO}^2}{\phi_{LO_{M\&N}}^2} = 1.36 + .0005P + .1\frac{G}{10^6} - .000714P\frac{G}{10^6}$$

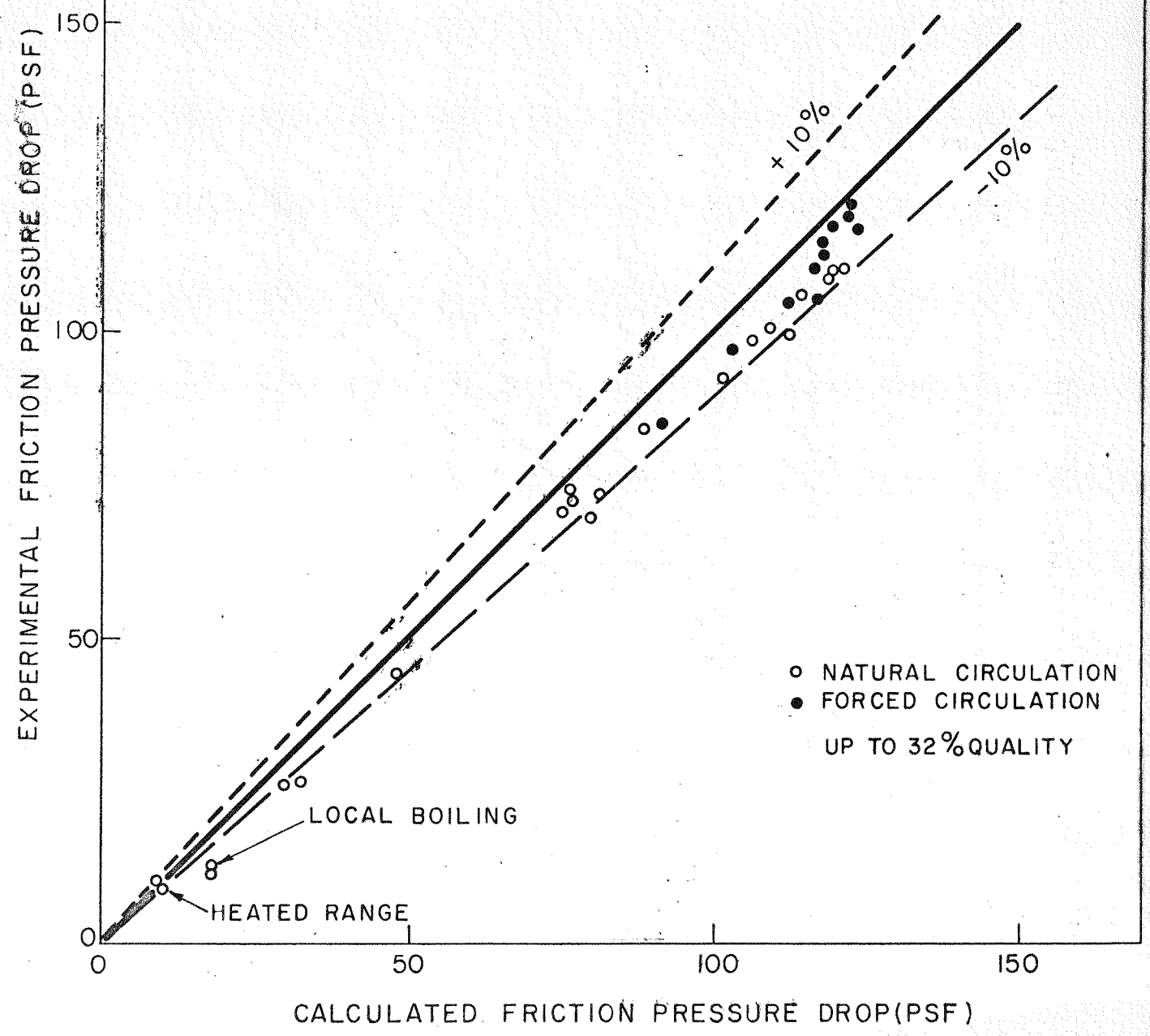

FIGURE 10

EXPERIMENTAL VS CALCULATED FRICTION PRESSURE DROPS WITH MASS VELOCITY DEPENDENCY

P=1200 PSIA
22" BETWEEN PRESSURE TAPS
109 °F INLET SUBCOOLING
0.210"X 1"X 27" CHANNEL

$$\frac{\phi_{LO}^2}{\phi_{LO}^2_{M\&N}} = 1.36 + 0.0005\,P + 0.1\frac{G}{10^6} - .000714\,P\,\frac{G}{10^6}$$

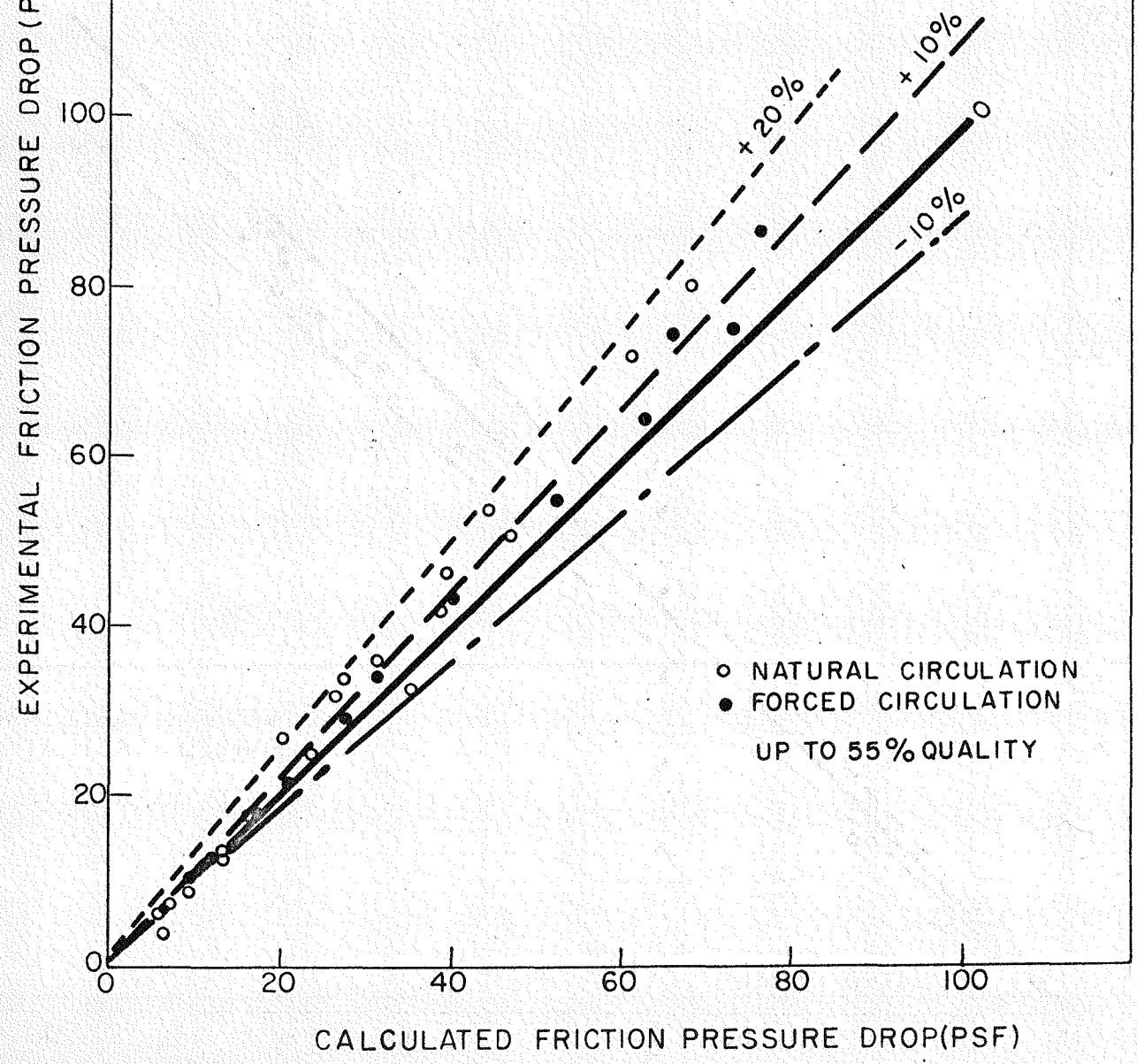

FIGURE 11

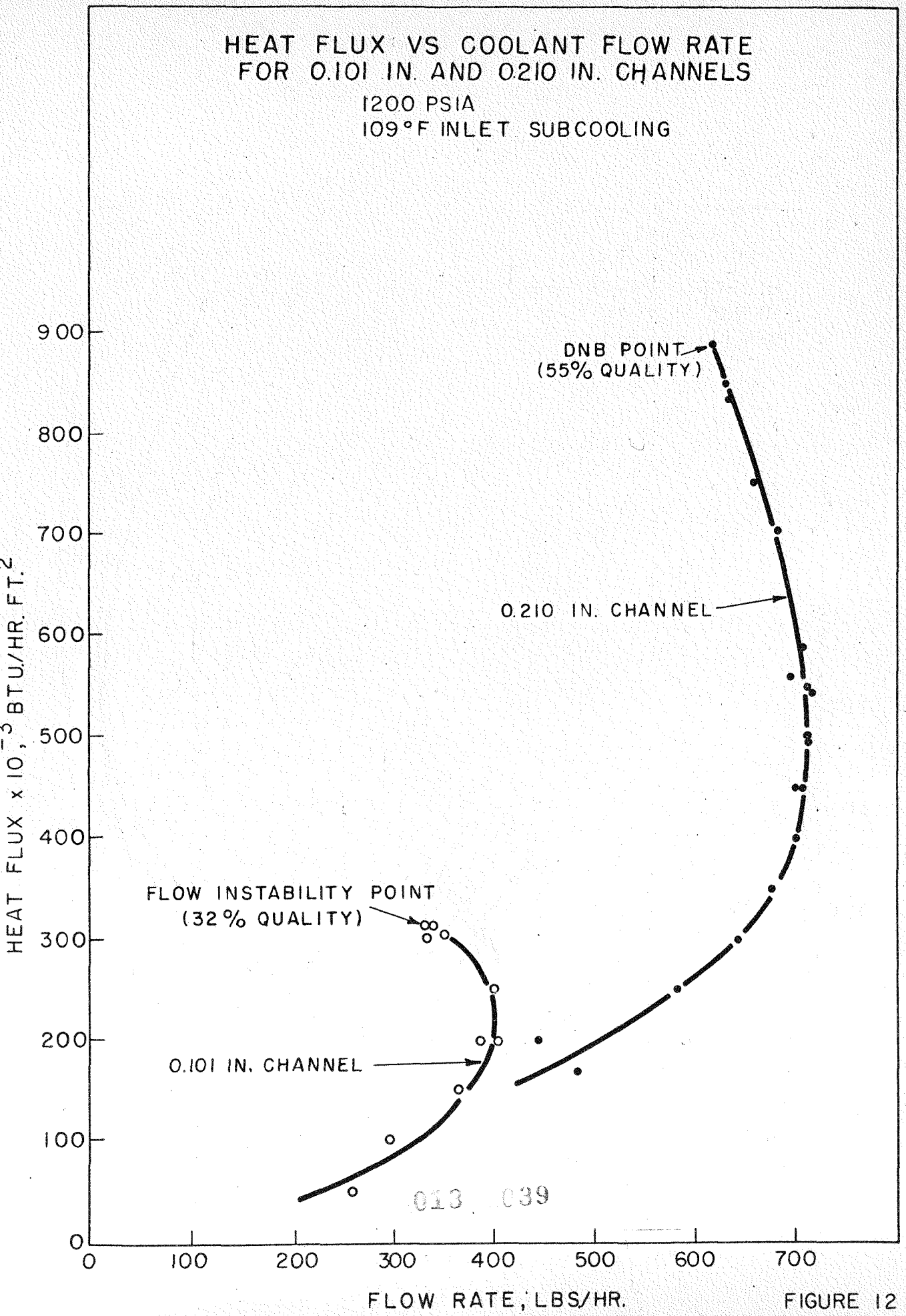
HEAT FLUX VS COOLANT FLOW RATE
FOR 0.101 IN. AND 0.210 IN. CHANNELS
1200 PSIA
109°F INLET SUBCOOLING
DNB POINT
(55% QUALITY)
0.210 IN. CHANNEL
FLOW INSTABILITY POINT
(32% QUALITY)
0.101 IN. CHANNEL
HEAT FLUX x 10,$^{-3}$ BTU/HR. FT.^{2}
FLOW RATE, LBS/HR.
0
100
200
300
400
500
600
700
800
900

FIGURE 12

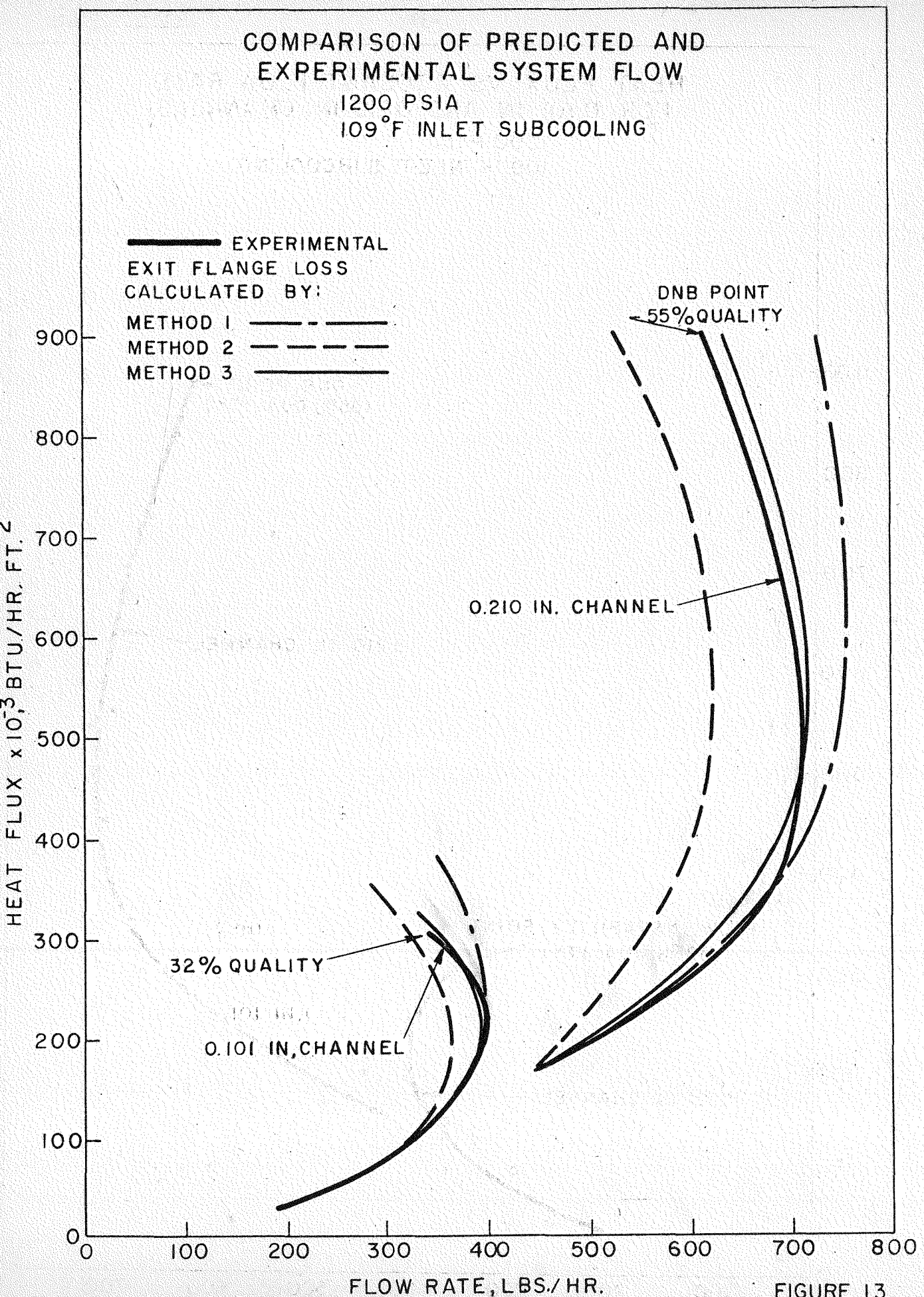

FIGURE 13

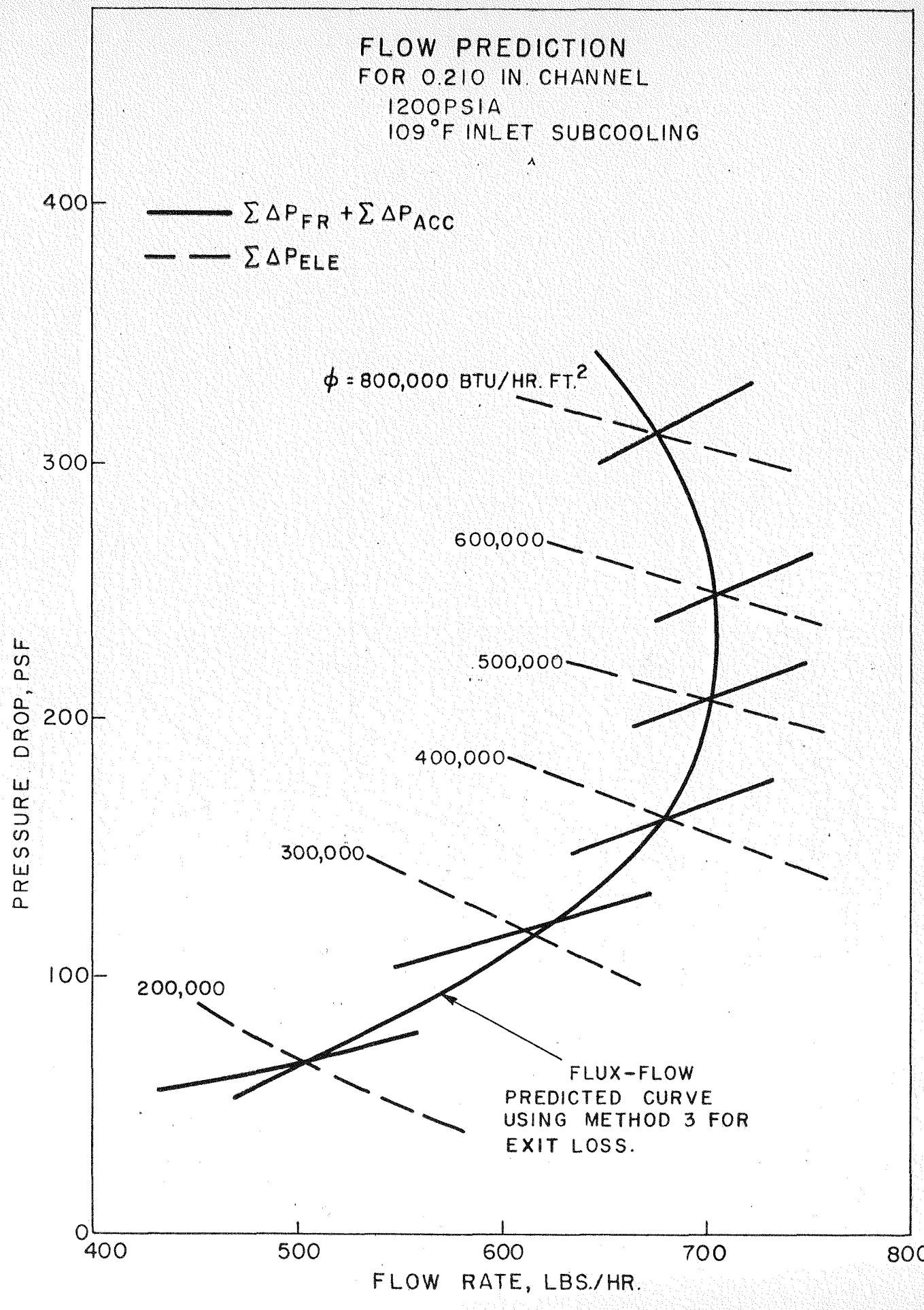
FLOW PREDICTION
FOR 0.210 IN. CHANNEL
1200PSIA
109°F INLET SUBCOOLING
$\Sigma \Delta P_{FR} + \Sigma \Delta P_{ACC}$
$\Sigma \Delta P_{ELE}$
ϕ = 800,000 BTU/HR. FT.^{2}
600,000
500,000
400,000
300,000
200,000
FLUX-FLOW PREDICTED CURVE USING METHOD 3 FOR EXIT LOSS.
PRESSURE DROP, PSF
0
100
200
300
400
400
500
600
700
800
FLOW RATE, LBS./HR.

FIGURE 14

OSCILLATORY BEHAVIOUR OBSERVED IN BETTIS NATURAL CIRCULATION LOOP #29

(PRELIMINARY RUN)

P = 1200 PSIA

ϕ = 320,000 BTU/HR-FT^2

INLET SUBCOOLING = 109°F

CHANNEL SIZE = 0.101" x 1" x 27"

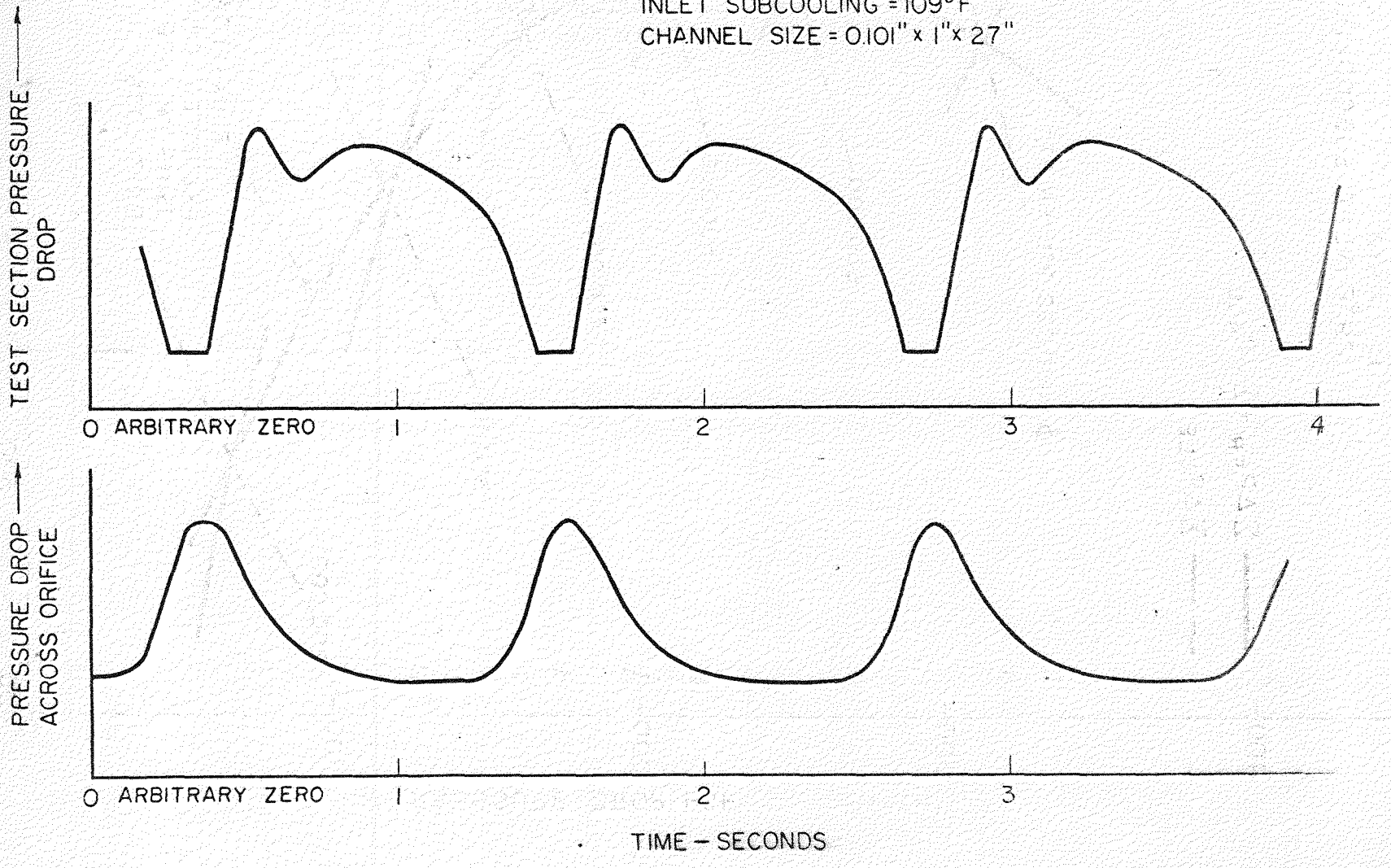

WAPD-AD-TH-470

APPENDIX A

Acceleration Pressure Drop

From Newton's second law, a one-dimensional model, and the continuity of matter, the acceleration forces are

$$d F_{acc} = \frac{dz}{g_c}\left[W \frac{\partial V}{\partial z} + A\rho \frac{\partial V}{\partial t} \right] \tag{A-1}$$

Dividing this into convection and time components

$$d F_{acc\ convection} = \frac{dz}{g_c} W \frac{\partial V}{\partial z} = \frac{W}{g_c} dV \tag{A-2}$$

$$d F_{acc\ time} = \frac{dz}{g_c} A\rho \frac{dV}{dt} = \frac{A\rho}{g_c} \frac{\partial V}{\partial t} dz \tag{A-3}$$

For steady flow, $\partial V/\partial t = 0$, and the acceleration pressure drop is

$$\Delta P_{acc_{1-2}} = \int_1^2 \frac{dF}{A} = \int_1^2 \frac{W}{gA_c} dV \tag{A-4}$$

But $W = AV\rho$, therefore

$$\Delta P_{acc_{1-2}} = \int_1^2 \frac{\rho V dV}{g_c} \tag{A-5}$$

For a change in area from 1 to 2 with constant density, equation (A-5) becomes

$$\Delta P_{acc_{1-2}} = \frac{\rho}{g_c} \int_1^2 V dV \tag{A-6}$$

integrating and substituting $V = \frac{W}{A\rho}$

$$\Delta P_{acc_{1-2}} = \frac{W^2}{2g_c\rho} \left[\frac{1}{A_2^2} - \frac{1}{A_1^2} \right] \tag{A-7}$$

For a change of density from 1 to 2 with constant area, equation (A-5) becomes

$$\Delta P_{acc_{1-2}} = \frac{W}{g_c A} \int_1^2 dV \qquad (A-8)$$

$$\Delta P_{acc_{1-2}} = \frac{W^2}{g_c A^2} \left[\frac{1}{\rho_2} - \frac{1}{\rho_1} \right] \qquad (A-9)$$

For both a change in density and in area over the same length the acceleration pressure drop is more difficult to find. This is the case in the riser because of the variable slip ratio with velocity. Using $W = \rho VA$ equation (A-5) becomes

$$\Delta P_{acc_{1-2}} = \frac{W^2}{g_c} \int_1^2 \frac{1}{A} d \left(\frac{1}{A\rho} \right) \qquad (A-10)$$

In Fig. 16 the area under the curve represents $\Delta P_{acc_{1-2}}$

(a) A = constant (Equation A-9)

(b) ρ = constant (Equation A-7)

(c) Neither = constant (Equation A-11)

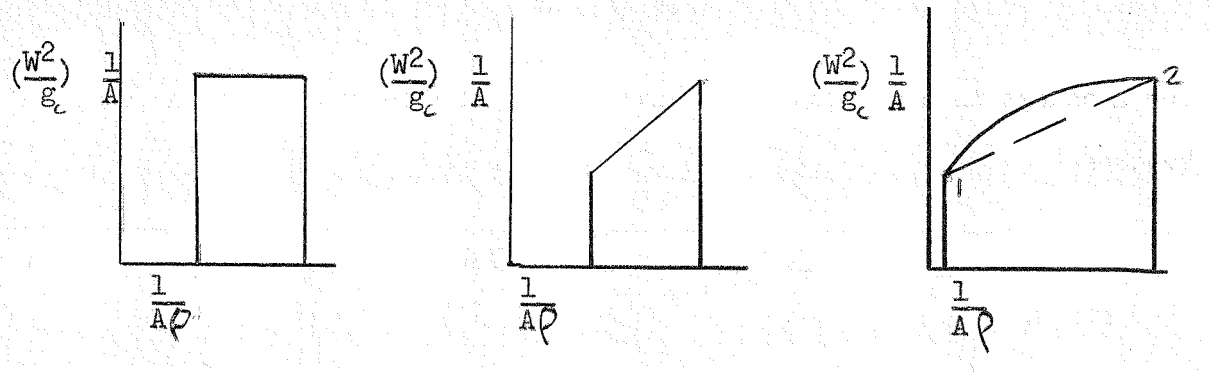

Fig. 16

For (16c) an approximation of the area is made by drawing a straight line between Points 1 and 2.

$$\Delta P_{accl-2} = \frac{W^2}{2g_c} \left[\frac{1}{A_2} + \frac{1}{A_1} \right] \left[\frac{1}{\rho_2 A_2} - \frac{1}{\rho_1 A_1} \right] \qquad (A-11)$$

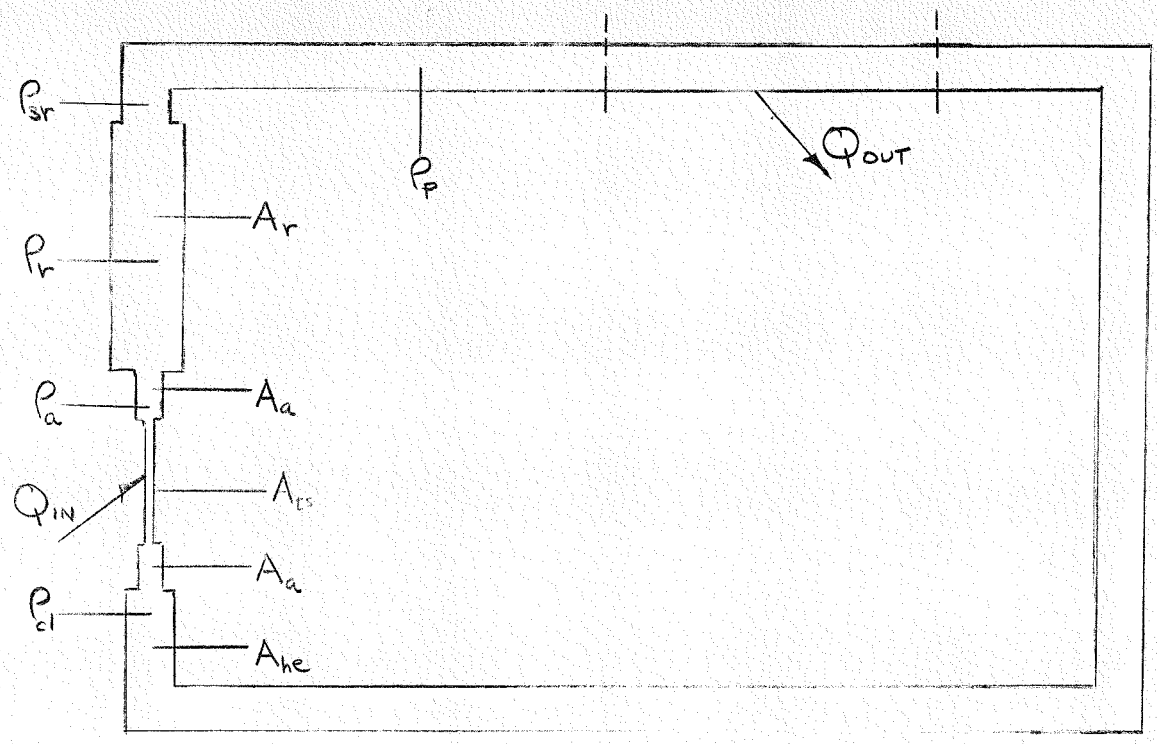

Fig. 17

Summing the acceleration losses around the loop (Fig. 17),

$$\Delta P_{\substack{acc \\ loop}} = \frac{W^2}{g_c}\left\{\frac{1}{2}\left[\frac{1}{\rho_{cl}A_a^2} - \frac{1}{\rho_{cl}A_{he}^2}\right] + \frac{1}{2}\left[\frac{1}{\rho_{cl}A_{ts}^2} - \frac{1}{\rho_{cl}A_a^2}\right] + \left[\frac{1}{A_{ts}^2\rho_a} - \frac{1}{A_{ts}^2\rho_{cl}}\right] + \frac{1}{2}\left[\frac{1}{\rho_a A_a^2} - \frac{1}{\rho_a A_{ts}^2}\right] + \frac{1}{2}\left[\frac{1}{A_r} + \frac{1}{A_a}\right]\left[\frac{1}{\rho_r A_r} - \frac{1}{\rho_a A_a}\right] + \frac{1}{2}\left[\frac{1}{A_{he}} + \frac{1}{A_r}\right]\left[\frac{1}{\rho_{sr}A_{he}} - \frac{1}{\rho_r A_r}\right] + \left[\frac{1}{\rho_p A_{he}^2} - \frac{1}{\rho_{sr}A_{he}^2}\right] + \left[\frac{1}{\rho_{cl}A_{he}^2} - \frac{1}{\rho_p A_{he}^2}\right]\right\} \quad \text{(A-12)}$$

Simplifying

$$\Delta P_{\substack{acc \\ loop}} = \frac{W^2}{2gA_{ts}^2}\left[\frac{1}{\rho_a} - \frac{1}{\rho_{cl}}\right] + \frac{W^2}{2gA_{he}^2}\left[\frac{1}{\rho_{cl}} - \frac{1}{\rho_{sr}}\right] + \frac{W^2}{2gA_rA_a}\left[\frac{1}{\rho_r} - \frac{1}{\rho_a}\right] + \frac{W^2}{2gA_rA_{he}}\left[\frac{1}{\rho_{sr}} - \frac{1}{\rho_r}\right] \quad \text{(A-13)}$$

APPENDIX B TABLE B-1

NATURAL CIRCULATION TEST DATA

Channel: 0.101 in. x 1.0 in. x 27 in.
20 in. between Test Section Taps

Test Section Pressure Drop (PSF)

Run	$\phi \times 10^{-5}$ Btu/hr-ft^2	W Lb/hr	$X_{Tap\ 2}$ X	T_{in} °F	T_{cl} °F	ρ_R Lb/ft^3	Total Meas.	Total Calc.	Friction Meas.	Friction Calc.	Calculated ΔP_{Acc}	Calculated ΔP_{Elev}	ΔP_{Ent}	ΔP_{Exit}
11-7	0.50	261	---	459	447	48.7	92.4	92.0	10.0	9.6	0.4	82.0		
11-8	1.00	295	---	459	467	46.0	92.3	98.1	12.1	17.9	0.8	79.4	Not Available	
12-1	1.49	365	0.011	458	449	44.2	106.7	111.1	25.4	29.8	3.1	78.2		
12-3	2.50	385	0.151	461	452	35.8	157.9	162.0	72.5	76.6	26.9	58.5		
12-4	3.05	349	0.275	459	461	32.0	184.0	196.7	99.1	111.8	39.0	45.9		
13-5	2.55	383	0.164	462	453	35.8	158.8	166.1	73.6	80.9	28.1	57.1		
13-6	3.01	349	0.268	459	450	32.7	184.9	193.0	100.6	108.7	37.7	46.6		
14-4	2.49	394	0.142	461	454	36.0	157.3	161.7	70.5	74.9	26.9	59.9		
14-5	1.99	404	0.065	461	457	39.8	130.9	134.9	44.1	48.1	15.8	71.0		
14-6	1.49	353	0.037	468	468	42.7	109.5	115.9	26.5	32.9	8.0	75.0		
14-7	0.98	297	---	462	466	46.2	92.1	98.2	11.8	17.9	0.8	79.5		
14-8	0.50	267	---	464	445	48.7	92.1	92.3	9.8	10.0	0.4	81.9		
16-4	2.53	376	0.166	462	463	36.0	154.0	164.1	69.8	79.9	27.5	56.7		
16-5	2.94	360	0.236	455	456	33.9	177.5	184.9	92.9	100.3	34.7	49.9		
16-6	3.14	337	0.305	459	460	32.2	187.8	199.6	105.1	116.9	39.3	43.4		
18-6	3.19	333	0.318	459	460	31.6	190.9	200.9	108.6	118.6	40.0	42.3		
18-7	3.16	332	0.322	460	463	31.6	191.3	201.71	109.7	120.1	39.7	41.9		
18-8	3.15	332	0.322	462	463	31.4	191.5	202.7	110.1	121.3	39.9	41.5		
19-1	3.06	328	0.310	460	463	31.7	186.3	194.5	105.9	114.1	37.6	47.8		
19-2	2.95	355	0.252	460	460	33.2	181.5	188.8	98.2	105.5	35.3	48.0		
19-3	2.77	374	0.193	456	455	34.2	169.3	173.4	84.0	88.1	30.9	54.5		
19-5	2.54	382	0.158	460	462	35.7	159.4	161.3	74.2	76.1	26.7	58.5		

APPENDIX B TABLE B-2

FORCED CIRCULATION TEST DATA

Channel: 0.101 in. x 1 in. x 27 in.
20 in. between Test Section Taps

Test Section Pressure Drop (PSF)

Run	$\phi \times 10^{-5}$ Btu/hr-ft^2	W Lb/hr	$X_{Tap\ 2}$ X	T_{in} °F	T_{cl} °F	ρ_R Lb/ft^3	Total Meas.	Total Calc.	Friction Meas.	Friction Calc.	Calculated ΔP_{Acc}	Calculated ΔP_{Elev}
19-6	2.75	374	0.056	459	459	35.1	169.9	175.7	84.9	90.7	31.4	53.6
19-7	2.94	355	0.250	458	458	33.4	181.2	186.8	97.0	102.6	35.4	48.8
20-1	3.16	312	0.354	462	465	31.4	198.7	200.2	120.8	122.3	39.1	38.8
20-2	3.19	335	0.312	456	459	31.6	195.2	200.5	112.5	117.8	39.7	43.0
20-8	3.19	343	0.303	458	462	31.6	201.2	203.3	117.1	119.2	40.5	43.6
21-1	3.15	343	0.308	464	465	31.8	199.9	206.5	116.5	123.1	41.0	42.4
21-2	3.05	333	0.299	460	461	32.1	187.7	195.8	104.4	112.5	39.6	43.7
21-3	3.10	330	0.314	460	464	32.0	190.9	197.2	110.0	116.3	38.5	42.4
21-4	3.15	330	0.317	459	462	31.9	195.6	199.1	114.2	117.7	39.0	42.4
21-5	3.17	329	0.329	462	464	31.6	199.8	203.2	118.7	122.1	40.0	41.1

WAPD-AD-TH-470

APPENDIX B TABLE B-3

NATURAL CIRCULATION TEST DATA

Channel: 0.210 in. x 1.0 in. x 27 in.
22 in. between Test Section Taps

Test Section Pressure Drop (PSF)

Run	$\phi \times 10^{-5}$ Btu/hr-ft^2	W Lb/hr	$X_{Tap\ 2}$ X	T_{in} °F	T_{cl} °F	ρ_R Lb/ft^3	Total Meas.	Total Calc.	Friction Meas.	Friction Calc.	Calculated / ΔP_{Acc}	Calculated / ΔP_{Ele}	ΔP_{Ent} 3-1	ΔP_{Exit} 9c-2
3-1	1.69	483	---	460	458	45.7	94.1	94.1	6.0	5.9	0.6	87.5	99.9	92.2
3-2	2.00	444	0.006	461	459	44.3	94.4	95.1	6.9	7.6	1.0	86.5	102.8	88.7
3-3	2.51	582	0.023	458	461	42.1	96.8	97.9	8.2	9.4	3.1	85.5	107.1	87.7
3-4	3.02	645	0.057	463	462	39.4	102.0	102.9	12.8	13.7	8.6	80.6	111.0	87.8
3-5	3.52	677	0.076	459	457	37.4	107.0	106.2	17.6	16.7	11.6	77.8	114.4	90.1
3-7	4.50	700	0.146	460	457	32.8	119.1	115.5	31.2	27.6	20.3	67.6	115.9	101.2
3-8	4.94	714	0.177	461	459	30.6	125.5	121.5	37.6	33.6	24.3	63.6	117.2	106.1
4-1	5.47	717	0.211	459	456	29.3	131.0	128.0	42.1	39.0	28.7	60.2	119.0	112.0
4-2	5.62	697	0.245	463	463	27.6	134.9	131.5	47.1	43.7	31.7	56.1	119.9	112.4
4-3	4.98	712	0.171	456	456	31.0	124.4	120.4	35.8	31.7	23.5	65.1	119.5	103.3
4-4	4.52	708	0.138	457	458	32.3	120.3	115.6	31.3	26.6	20.0	69.0	118.6	97.7
4-5	3.98	702	0.097	457	456	34.4	116.8	110.5	26.6	20.2	15.3	74.9	117.8	82.3
4-6	5.49	713	0.216	459	457	28.5	135.5	128.3	46.8	39.6	29.0	59.7	119.3	110.6
4-7	5.89	708	0.248	458	456	26.9	144.4	134.8	54.1	44.5	33.8	56.5	119.3	115.7
5-1	7.04	681	0.365	460	458	23.6	163.1	151.8	72.3	61.0	44.4	46.4	122.0	117.5
5-2	7.54	660	0.430	462	463	21.8	172.5	160.0	80.4	67.9	50.0	42.1	117.2	123.8
5-4	8.52	631	0.544	461	462	19.7	---	177.2	---	79.1	61.8	36.2	117.0	123.6
5-5	8.36	634	0.524	459	458	20.4	---	173.2	---	76.5	59.3	37.4	115.7	---
10-1	1.99	465	0.026	459	450	42.4	90.4	93.7	3.1	6.5	2.2	85.1	142.8	81.4
10-2	2.99	520	0.109	460	457	35.4	94.7	95.7	12.5	13.6	9.4	72.8	174.7	76.0
10-3	4.01	569	0.180	459	457	31.3	104.2	102.7	25.0	23.5	15.7	63.5	186.8	79.4
10-4	5.01	597	0.255	459	458	28.9	112.6	115.1	32.6	35.1	24.3	55.7	189.6	85.9
10-5	5.95	601	0.342	460	459	24.3	131.0	127.2	50.8	46.9	32.3	47.9	186.5	91.3
10-6	7.00	599	0.442	460	457	21.6	149.9	144.0	65.5	59.6	42.6	41.8	186.4	95.3

APPENDIX B TABLE B-4

FORCED CIRCULATION TEST DATA

Channel: 0.210 in. x 1.0 in. x 27 in.
20 in. between Taps

Test Section Pressure Drop (PSF)

Run	$\phi \times 10^{-5}$ Btu/hr-ft^2	W Lb/hr	$X_{Tap\ 2}$ X	T_{in} °F	T_{cl} °F	ρ_R Lb/ft^3	Total		Friction		Calculated			
							Meas.	Calc.	Meas.	Calc.	ΔP_{Acc}	ΔP_{Ele}	ΔP_{Ent}	ΔP_{Exit}
6-3	1.93	488	0.008	460	---	45.4	93.9	94.3	6.4	6.6	1.0	86.5	102.1	93.9
6-5	2.50	584	0.023	458	---	41.8	98.4	98.0	9.9	9.4	3.0	85.5	107.4	87.7
6-6	3.02	647	0.047	459	---	39.9	103.0	103.1	12.8	13.0	8.0	82.2	112.6	88.0
6-7	3.47	680	0.078	463	---	36.7	106.8	105.7	18.7	17.6	11.9	76.2	115.5	87.5
6-8	3.95	709	0.100	459	---	35.0	111.7	111.1	21.7	21.0	15.6	74.4	118.6	92.1
7-1	4.47	709	0.142	461	---	32.5	117.4	116.1	29.0	27.8	20.4	68.0	118.6	99.3
7-2	4.97	725	0.164	457	---	31.1	123.7	121.1	34.3	31.7	23.6	65.8	119.3	107.3
7-3	5.47	725	0.210	460	---	29.2	132.1	129.1	42.9	39.9	29.2	60.0	120.9	114.6
7-4	6.48	701	0.300	458	---	25.8	146.5	143.3	55.7	52.5	39.1	51.7	120.9	111.2
7-5	7.12	727	0.339	462	---	23.3	158.2	156.6	64.6	63.0	45.4	48.2	122.7	136.1
7-6	7.50	666	0.414	459	---	21.5	167.4	158.1	75.1	65.8	48.7	43.6	116.6	129.4
7-7	7.99	653	0.480	460	---	19.9	169.9	168.3	75.0	73.3	55.3	39.6	115.6	133.4
7-8	8.30	642	0.510	460	---	18.8	183.9	173.0	87.2	76.3	58.7	38.0	116.3	135.6

REFERENCES

1. Mendler, O. J., "Status Report of the Natural Circulation Testing Program," WAPD-TH-460, October, 1958.
2. "Forced-Convection Heat Transfer Burnout Studies for Water in Rectangular Channels and Round Tubes at Pressures above 500 Psia.," WAPD-188, October, 1958.
3. Troy, M. "Upflow Burnout Data for Water at 2000, 1200, 800 Psia, and 600 Psia in Vertical 0.070 in. x 2.25 in. x 72 in. Long Rectangular Channels." WAPD-TH-408.
4. Rathbun, A. S., "Flow Distribution in a Parallel Channel, Pressurized Water Reactor-Code Development and Parameter Effect," WAPD-T-663, Presented at June, 1958 ANS Meeting, January, 1958.
5. LeTourneau, B. and Troy, M., "Heating, Local Boiling, and Two-Phase Pressure Drop for Vertical Upflow of Water at Pressure below 1850 Psia; Test Data and Correlations," WAPD-TH-410, 1958.
6. Sher, N. C., "Estimation of Boiling and Non-Boiling Pressure Drop in Rectangular Channels at 2000 Psia," WAPD-TH-300, 1957.
7. Martinelli, R. C. and Nelson, D. B., Prediction of Pressure Drop during Forced-Circulation Boiling of Water, Trans. ASME, 1948 70:695-705.
8. Sher, N. C., "Review of Martinelli and Nelson Pressure Drop Correlations," WAPD-TH-219, July, 1956.
9. Marchaterre, J., "Effect of Pressure on Boiling Density in Multiple Rectangular Channels," ANL-5522, February, 1956.
10. Kays, W. M. and London, A. L., "Compact Heat Exchangers" National Press, 1955.